Alma Mater Studiorum – Università di Bologna

DOTTORATO DI RICERCA IN

INGEGNERIA AGRARIA
Ciclo XXV

Settore Concorsuale di afferenza: 07/C1

Settore Scientifico disciplinare: AGR09

TITOLO TESI

APPLICATIONS OF INFRARED THERMOGRAPHY IN THE FOOD INDUSTRY

Presentata da: LUCIAN CUIBUS

Coordinatore Dottorato **Relatore**

Prof. Ing. Adriano Guarnieri **Ing. Angelo Fabbri**

Dr. Luigi Ragni

Esame finale anno 2013

“Learning is experience. Everything else is just information.”

Albert Einstein

CONTENTS

INDEX OF FIGURES

INDEX OF TABLES

INTRODUCTION

In the last 20-30 years, the implementation of new technologies from the research centres to the food industry process was very fast. Normally, the technological developments add value to stimulate the agricultural production, industrial processing and services. In this direction all the companies try to implement new technologies to reduce the cost of energy respecting also the environmental rules. The further distinguished characteristics of the food industry are the technological and economic relations. Almost all the industrial food processors have to use the thermal process to obtain an optimal product respecting the quality and safety standards.

Non-contact and non-destructive methods are increasingly used in the present in the food industry because of the benefit provided by them. The infrared thermography has been used in a small part of the food industry because of its high price and the difficulty of using. The recent infrared thermocamera, the new software and the lower prices simplified the applications in the industrial field. Thermography has now a higher applicability in the food industry because it is a non-contact technique and also totally non-destructive. This confers a big advantage for the processors saving time, energy and a reduction of cost.

The present work is divided in two big chapters.

The science of thermography and also some applications made in the past by other researchers were described and presented in the first chapter. In the second chapter, the researches made on the different food products that can help the food industry were presented.

I. INFRARED THERMOGRAPHY IN THE FOOD INDUSTRY

I.1 The science of infrared thermography

Infrared thermography (IRT) or thermal imaging is a rapid, non-contact and non-destructive powerful technique to determine the defects, changes near-surface of different products, by measuring the surface temperature. The etymology of the word "Thermography" derived from "thermo" and "graphy", the Greek origin words, "thermē" that means heat, warm, and "graphein" that means graphic, writing and literally we can say that thermography is "writing with heat". This technique involves the detection of electromagnetic radiation, the invisible infrared pattern emitted by the surface objects, and the conversion of this into a visible image - "thermogram" (Vavilov 1992; Carino 1994; Rao 2008; Vadivambal & Jayas 2010). In fact this technique is like taking photographs but with a camera having an infrared detector.

The classical instruments like thermometers, thermocouples, thermistors, and resistance temperature detectors can measure the temperature only at specific point and most of these instruments need a contact with material (Meola 2004, Vadivambal & Jayas 2010). The thermography revolutionized the concept of measurements and temperature monitor and this can be very useful for many fields that require a non-contact method and a bigger area to determine the temperature of the products (Omar 2005; Vadivambal & Jayas 2010).

The first mentions of existence of invisible thermal rays had been hypothesized by Titus Lucretius Carus (c.99 – c. 55 BCE), a roman poet and the author of the philosophic epic "De Rerum Natura" ("On the Nature of the Universe") (Vavilov 1992). In 1800,3 the Sir William Herschel, English royal

astronomer and physicist of King George III, discovered the first thermal radiation, infrared radiation outside the deep red in the visible spectrum, the invisible light later called infrared (Herschel 1800, Vavilov 1992, Meola 2004). The son of Sir William, Josh Hershel, proposed an evaporograph like a prototype of IR imagers that focused with a lens solar radiation onto a suspension of carbon particles in alcohol. In 1840 he called a thermal image "thermogram", term still in use today (Vavilov 1992). As a result of the next studies and observations of others scientists like Macedonio Melloni, Gustav Kirchhoff, James Clerk Maxwell, Joseph Stefan, Ludwig Boltzmann, Max Planck, Albert Einstein, and others contributed to a fast progress of infrared thermography that become an important technique to determine the surface temperature of the objects (Vavilov 1992; Meola 2004). In 1954 a real prototype of an airborne opto-mechanical IR imager was developed in the USA and was an important step for the development of Forward Looking Infrared (FLIR) systems mounted on aircraft (Vavilov 1992). After the military application used in World War II, more technology was developed for many fields like aerospace industry, civil structures, medicine, agriculture and food industry, non-destructive evaluation, environmental and others (Vavilov 1992; Omar 2005). Thermal non-destructive testing (TNDT) is a particular application area of IR thermography with its own history. One of the first industrial applications of TNDT was related to analysis of hot rolled metal by Nichols on 1935 (Vavilov 1992). This technique was also used in the civil engineering to detect the corrosion-induced delaminations in reinforced concrete bridges decks in North America, where in the late 1970s, Virginia Highway and Transportation Research Council (Clemeiia & McKeel, 1978) and the Ontario Ministry of Transportation and Communication (Manning and Holt, 1983) do the

early research independently (Carino 1994). This initial studies involved handheld scanners and photographic cameras to record the thermographic images (Carino 1994). In *figure 1* we can see a scheme with the important components of an infrared thermocamera.

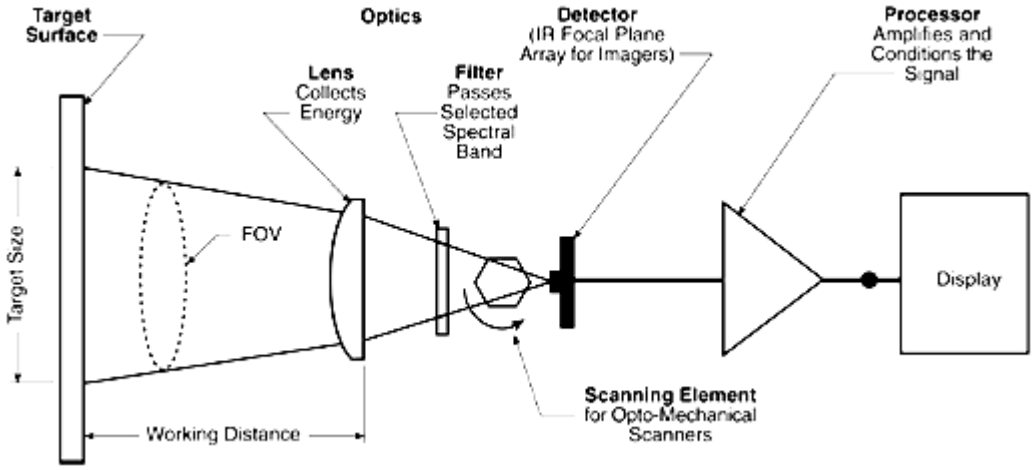

Figure 1 Components of an Infrared Sensing Instrument (Zayicek 2002)

The infrared radiation (IR) is not detectable by the human eye, and the most important element of IR camera is the radiation receiver called detector. The infrared thermocamera detector is a focal plane array (FPA) of micrometer size pixels made of various materials sensitive to IR wavelengths. The resolution of FPA starts from 160 x 1120 pixels up to 1024 x 1024 pixels (Flir, 2010). We have 2 categories of infrared detectors: *quantum detectors* and *thermal detectors*. The quantum detectors are faster (ns to μs) and more sensitive than thermal detectors, because they are based on photon detector, the radiation is absorbed within the material by interaction with electrons (Chrzanowski & Rogalski 2006). But unfortunately to archive this information quantum detectors require cryogenic cooling and this is the main obstacle to the more widespread use of this detectors.

The bolometer was invented by the American astronomer Samuel Pierpont Langley at 1878. The bolometers have a temperature dependency and they measure electrical resistance. The changes of temperature can be measured directly or via an attached thermometer. The most used and cheap thermal detector is a microbolometer, a special detector for measuring the energy of incident electromagnetic radiations. The infrared radiation wavelengths between 7-14 μm strikes the detector material, heating it, and thus changing his resistance. This electrical resistance is measured and processed into temperatures to create an image – thermogram. In the last period, thermal detectors are more exploited in commercial systems because they are cheaper, do not require cooling and can be obtained good imagery. The speed and the moderate sensitivity of thermal detectors are quite adequate for nonscanned imagers with two-dimensional (2D) detectors. The performance of a thermocamera is determined by the quality of the thermal image and the temperature resolution.

Large arrays of thermal detectors could help reach the best values of noise equivalent differential temperature (NETD), below 0.1 K, due to effective bandwidths less than 100Hz. It can be shown that the temperature sensitivity of an imager, the so-called noise equivalent temperature (NETD), can be given by (Lloyd, 1975):

$$NETD = \frac{4 f_{\#}^{2} (\Delta f)^{1/2}}{A^{1/2} t_{op} M^{*}} \qquad \text{(I.1.)}$$

where $f_{\#}$ is the *f*-number of the detector optics ($f_{\#} = f/D$, f is the focal length and D the diameter of the lens), t_{op} the transmission of the optics and M^{*} the figure of merit that includes not only the detector performance D* but also the spectral

dependence of the emitted radiation, ($(\partial S / \partial T)_\lambda$), and the atmospheric transmission t_{at}, it is given by following equation:

$$M^* = \int_0^\infty \left(\frac{\partial S}{\partial T} \right)_\lambda t_{at\lambda} D_\lambda^* d\lambda \qquad \text{(I.2.)}$$

NETD of one detector is the difference of temperature of the object required to produce an electric signal equal to the rms (root mean square) noise at the input of the display (Rogalski 2000).

The infrared electromagnetic radiation is located in the infrared electromagnetic spectrum like we can see in the *figure 2*. Infrared radiation covers a portion of the electromagnetic spectrum from approximately 700 to 14.000 nanometres (0.7-14 µm). All the objects emitted infrared radiation above absolute zero (0 kelvin = -273, 15°C), and the amount of radiation increased with temperature. The intensity of object radiation is directly correlated with the temperature distribution on the surface of the object, and depends also on the surface condition, thermal properties of the material and the environment (Weil 1992).

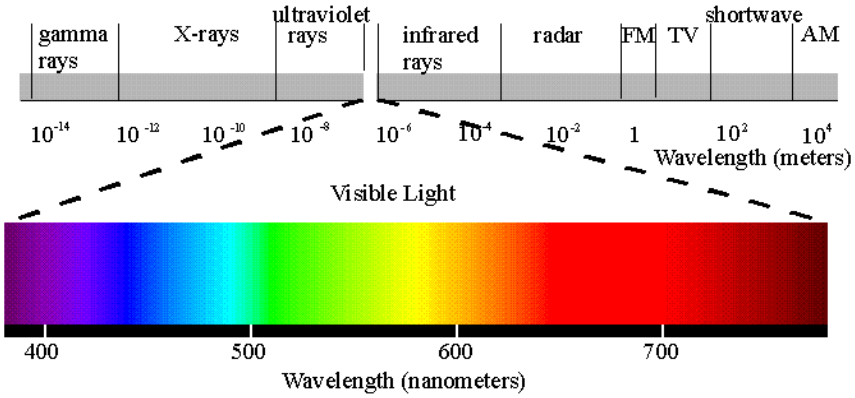

Figure 2. Electromagnetic Spectrum (Kaiser 1996)

Following the works of Planck, Stefan, Boltzmann, Wien, Rayleigh and Kirchhoff, they defined precisely the electromagnetic spectrum and established quantitative and qualitative correlations describing the infrared energy. The objects are composed of continually vibrating atoms, with higher energy atoms vibrating more frequently and this vibration of all particles generates electromagnetic waves. The higher temperature of an object is, the faster vibration, and thus the higher the spectral radiant energy (Chrzanowski & Rogalski 2006). The measurement of thermal infrared radiation is the basis for non-contact temperature measurement and thermal imaging (or thermography) (Zayicek 2002). All the objects are continually emitting radiation at a rate with a wavelength distribution that depends upon the temperature of the object and its spectral emissivity $\varepsilon(\gamma)$ (Chrzanowski & Rogalski 2006). The process of thermal infrared radiation leaving a surface is called exitance or radiosity. (Zayicek 2002). One object reacts to incident radiations from its surroundings by absorbing, reflecting, or transmitting, passing through (as through a lens) as illustrated in *figure 3*.

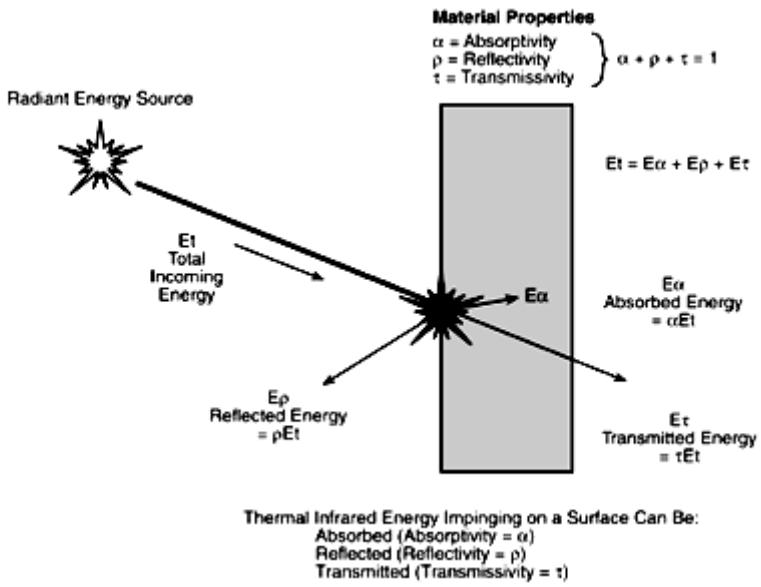

Figure 3 Radiation exchange at the target surface (Zayicek 2002)

Kirchhoff's law states that the sum of the three components is always equal to the received radiation (the percentage sum of the three components equals' unity):

$$W = \alpha W + \rho W + \tau W, \quad (I.3.)$$

This can be simplified to:

$$1 = \alpha + \rho + \tau \quad (I.4.)$$

where W is total radiation, α is the absorption, ρ is reflection and τ transmission. Radiant emission is usually treated in terms of the concept of a blackbody, a theoretical ideal emitter (Ross 1994, Chrzanowski & Rogalski 2006). A blackbody is an object capable of absorbing all incident radiation at any wavelength and conversely, according to the Kirchhoff law, is a perfect radiator.

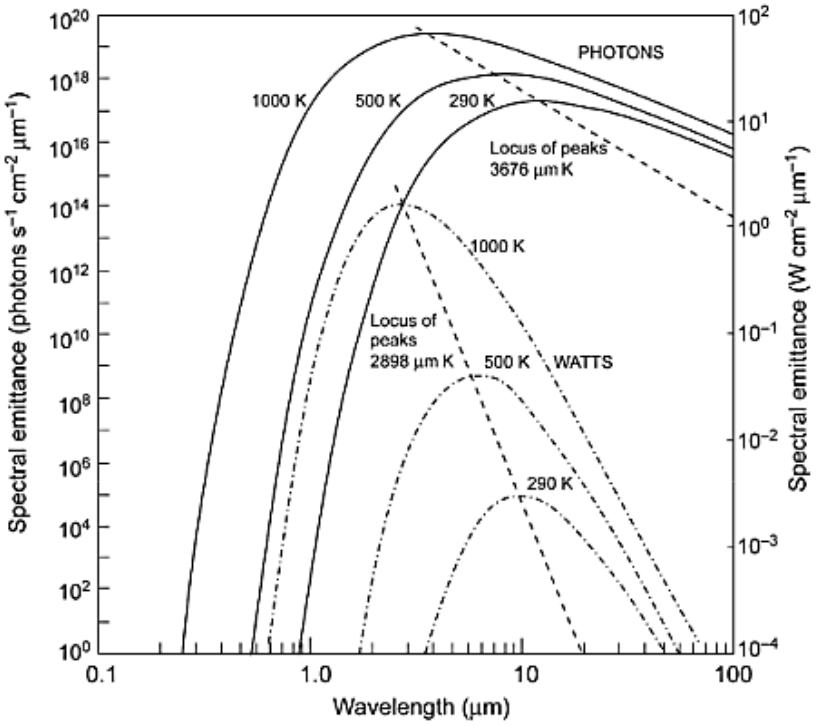

Figure 4 Planck's law for spectral emittance (Burnay et al., 1988)

The energy emitted by an ideal blackbody is the maximum theoretically possible for a given temperature. The radiative power (or number of photons emitted) and its wavelength distribution is given by the Planck radiation law (Chrzanowski & Rogalski 2006):

$$Wb(\lambda,T) = \frac{2\pi hc^2}{\lambda^5}\left[\exp(\frac{hc}{\lambda kT}) - 1\right]^{-1} \text{ W cm}^{-1}\mu\text{m}^{-1} \text{ (I.5.)}$$

where *Wb* (W $cm^{-1}\mu m^{-1}$) energy radiated per unit volume by a cavity of a blackbody in the wavelength interval, λ (μm) is the wavelength, *T* (K) the absolute temperature of a blackbody, *h* (6.6×10^{-34} Joule sec) Planck's constant, *c* (3×10^8 m/s) the velocity of the light and *k* (1.4×10^{-23} Joule/K) Boltzmann's constant. We can see a plot of these curves for a number of black body temperatures in the *figure 4.*

By differentiating Plank's law (Eq. I.5) with respect to λ and looking for the maximum radiation intensity, Wien's displacement law is obtained Eq. I.6. (Mayer & Feldmann 2001, Mori & all 2008):

$$\lambda_{\max} = \frac{2898}{T}[\mu m] \qquad \text{(I.6.)}$$

For an ideal black body absolute temperature T and λ (wavelength of maximum energy radiation) is a constant. By integrating Planck's formula from λ = 0 to λ = ∞, we obtain the total radiant emittance (Wb) for an idealized blackbody:

$$Wb = \sigma T^4 \left[Watt / m^2\right] \qquad \text{(I.7.)}$$

For real objects is not valid this law of Planck (for an idealized black body – perfect energy absorber), and was introduced the emissivity (ε):

$$W = \varepsilon \sigma T^4 \left[Watt / m^2\right] \qquad \text{(I.8.)}$$

Emissivity is a very important characteristic of a target surface and must be known in order to make accurate non-contact temperature measurements. The emissivity can be defined like the ratio of energy radiated from a product/object to the exterior and energy radiated from a black body. The value of emissivity is proportional to the radiant energy emitted by a product surface. The energy radiated is an indicator of the emitting of an object, and also the temperature of that.

In order to determine the temperature of an object, using the thermal imaging, the total radiant emittance and the emissivity of the object are both required. (Kolzer, Oesterschulze & Deboy, 1996; Gowen & all, 2010).

Emissivity or emittance is defined as the ratio of energy emitted from an object to the exterior, to that of a black body at the same temperature. Emissivity can vary from 0 (perfect white body) to 1 (perfect black body) (Gowen & all, 2010). The emissivity depends on: the composition of material, the geometry, the surface type and roughness. Usually the materials have an emissivity ranging from 0.1 to 0.99. For objects made of metal the emissivity is low increasing with temperature, and for non-metals objects it tends to be high, nearby 1 and decreases with temperature. The biological products normally have the emissivity nearby 1, same like the human skin (Flir, 2010).

The infrared thermocamera converts the energy emitted by an object into electrical signal via IR detectors, and displays it as a thermal image (colour or monochrome); this we can estimate the surface temperature of objects.

We can obtain the thermal images using the most used and important methods: **passive** or **active thermography** systems (classified by the source of heating of the object). We can talk about the passive thermography when the body of the object is heated by ambient conditions (solar radiation) (Rao, 2008).

In the active thermography the object is heated by an external source to obtain the contrast of temperature. Normally the passive thermography is used for assessing the large bodies like buildings, bridges, while active thermography is generally adopted in research centres and for different industrial processes (Rao, 2008). The thermal information obtained in the passive mode largely describes surface thermal properties (Gowen, 2010) Regarding the active thermography we have different techniques for generating thermal energy like *lock-in thermography* (expose to infrared radiation), *pulsed-phase thermography* (repeated heating at short intervals of time), *impulse thermography* (local heating),

vibrothermography (expose to sonic waves) (Rao, 2008, Maldague, Galmiche, & Ziadi, 2002, Shepard, Ahmed, & Lhota, 2004, Gowen & all, 2010)

Lock-in thermography, known as "modulated thermography", requires a thermal excitation applied to the sample surface to generate thermal waves. The infrared thermocamera can monitor the sample during the modulated excitation, measuring the resultant oscillating temperature field (Maldague, Galmiche, & Ziadi, 2002, Sakagami & Kubo, 2002, Gowen & all, 2010). Using a sinusoidally varying light source like laser beam, halogen lamp etc. the method is known as "optically excited lock-in thermography" (Gowen & all, 2010). If we can observe on the surface of the sample one uniformed temperature rise, then the sample doesn't have any defects; on the contrary, if we can observe regions with high temperature, those areas correspond to the areas where the defects of a sample are. (Sakagami & Kubo, 2002). As a consequence, the temperature distribution on the sample surface is used to estimate the location, shape and the size of the defects (Sakagami & Kubo, 2002).

The **pulsed-phase thermography** (PPT) combines the pulsed acquisition procedure with phase/frequency concepts of lock-in thermography for which specimens are submitted to a periodical excitation. This method was introduced for non-destructive evaluation in infrared thermography applications a few years ago as an interesting signal processing technique (Maldague et al., 2002).

To estimate the phase between the applied energy and local thermal response, this two techniques (lock-in and pulsed-phase thermography), use the Fourier transform on each pixel level of the time series of thermal images (Sakagami & Kubo, 2002, Gowen & all, 2010, Maldague et al., 2002).

Impulse thermography method requires an internal or external local heating of the sample; the heated part is observed by the infrared thermocamera to record the temperature change at the surface as a function of time. This method is more useful in civil engineering where we can detect defects like the voids, cracks in concrete, in tendon ducts and more (Maierhofer & all, 2006).

These considerations define the use of vibrothermography as a non-destructive method for observing the energy-dissipation ability of granular material. A scanning camera was used, which is analogous to a television camera. It utilizes an infrared detector system in a sophisticated electronics system in order to detect radiated energy, and to convert it into a detailed real-time thermal picture in a video system both colour and monochromatic. Response times are shorter than a microsecond.

Vibrothermography is used as a non-destructive method for observing the energy-dissipation ability of granular material, employs sonic waves to impart energy to the target surface. Flaws such as cracks and inclusions within a target resonate at the applied sonic frequency, resulting in localised heating. One advantageous feature of this technique compared with other methods of active thermography is that the bulk of the sample is not heated; therefore, contrast between flaws and surrounding material is increased (Shepard, Ahmed, & Lhota, 2004; Loung, 2007; Gowen & all, 2010).

According with Vavilov, 1992 all the IR imagers can be classified by application areas as follows:

1) simple imaging units used for night vision in military, IR reconnaissance, search and rescue, observation, fire fighting, technical diagnostics

etc., such as PalmIR-250 from Raytheon, Night Conqueror from Cincinnati Electronics etc.;

2) radiometric (temperature measuring) imagers used in technical diagnostics and non-destructive testing (general-purpose IR cameras and modules, such as ThermaCAM P60 and ThermoVision A40 from FLIR Systems, TH-9100 Pro from NEC Avio, Testo-880 from Testo etc.);

3) radiometric computerized IR thermographic systems mainly intended for scientific research and characterized by the highest temperature sensitivity and frame frequency, such as ThermaCAM SC 6000 from FLIR Systems and SC 7000 from FLIR-CEDIP. (Vavilov 1992)

Regarding IR imagers performance, a definite trend is further improvement of temperature and spatial resolution and increase of frame frequency. This non-destructive method will become more efficient and flexible to test different objects with different geometry.

I.2 Research concerning past and recent application of thermography in the food industry

The infrared thermography is a technique used recently for agriculture and food industry, in the past it was developed only for military applications and the price for this device was cost-prohibitive and no portable versions existed. In the last 10-15 years the prices for the sensors of infrared thermocamera decreased drastically and the producers created small portable versions for field measurement.

In food industry we know that the heating process has a major importance's to obtain a good and safe product with a long shelf life. Also we know that the traditionally way to measure and monitor the temperature with different methods (thermometers, thermocouples, thermistor) provide only a limited information's.

The thermal imaging has revolutionized the concept of temperature measurement in industries, and also in agriculture and food industry, because is a very helpful tool to be exploited for the assessment of manufacturing procedures as well for non-destructive evaluation of either end products, is fast, and also is a non-contact analysis (Vavilov, 1992, Gowen & all, 2010, Vadivambal & Jayas, 2010).

The recent research shows the potential of IRT for agriculture and food safety and quality assessment such as temperature validation, bruise and foreign body detection, grain quality evaluation, assessing the seedling viability, estimating soil water status, estimating crop water stress, scheduling irrigation, determining disease and pathogen affected plants, estimating fruit yield,

evaluating maturity of fruits and vegetables and more over (Vadivambal & Jayas, 2010, Gowen & all, 2010).

In 1999 Nott & Hall used infrared thermal imaging for mapping the temperature distributions induced by microwave in situ in two dimensions with good results in spatial resolution. The advantage of this technique is the non-invasive properties (can be applied to real food system without alterations), and the disadvantage is that it only provides a surface measurement from which the temperature within the sample has to be inferred in opinion of the same researchers (Nott & Hall, 1999).

The spatial and temporal temperature distribution patterns obtained from an object could have a potential application for food industry, for quality assurance, safety profiling and authenticity. Du & Sun conclude that the necessity of computer-based image processing technique is a consequence of increasing demands for consistency and efficiency within the food industry.

In scientific literature we can discover only some research in the food sector where thermal imaging was used. In the following paragraphs, I will present briefly this recent advances and the potential of application of infrared thermography for the food industry.

Advance and potential applications of thermal imaging to monitor the surface temperature of food product cooked in a microwave oven, in the spectral range of 8-12 μm, was reported by Goedeken, Tong, and Lentz (1991).

Others researchers, like Ibarra et al. (1999) applied this technique using a spectral range of 3.4 - 5 μm to control the heating and cooling cycles at the surface of food samples. They created a statistical model to express the internal temperature of breast chicken in terms of the external temperature and time. They

obtained an accuracy of ± 1.22°C for cooling times between 0 and 450 s, and ± 0, 55 °C after cooking. This research confirms that thermal imaging has a good potential for the real-time determination of the internal temperature of cooked chicken meat in industrial line to verify that the minimum endpoint temperature has been achieved.

Workmaste et al, (1999) used the infrared thermography to study the ice nucleation and propagation in plants and confirmed that the technique can be useful for studying the freezing process of plants.

Costa et al. (2007) used the infrared thermography on the slaughter-line for the assessment of pork and raw ham quality. They obtained good results when evaluating the meat and ham, using surface temperature differences. They analyzed 40 carcasses of heavy pigs at 20 min. after stunning, thus left and right caudal and dorsal surface images were kept for each half carcass. The settings of the camera were as follows: emissivity of pig's skin 0.98; reflected air temperature 22°C; distance between camera and skin surface m 2.5. These studies confirm the absence of relationship between meat quality traits and the skin surface temperature. The ham with a lower fat cover has a surface warmer surface. The preliminary results show a possible application of this technique for a good selection of raw hams destined to the successive dry-cured processing.

Others researches concerned to facilitate the control of heating and cooling cycles on surface of different food samples, for example the apparatus realized by Foster, Ketteringham, Swain et al., 2006. They design and develop an apparatus to provide repeatable surface temperature-time treatments on inoculated food samples using thermal imaging camera for temperature measurements. Temperature control to a defined ramp was achieved at an average accuracy of 1.7

°C and 2.4 °C on the sample surface, during heating and holding periods, respectively (Foster, Ketteringham, Swain et al., 2006).

Manickavasagan, Jayas, White, and Jian (2006), studied the application of thermal imaging for detection of hot spots in grain storage silos; the existence of non-contact method to detect hot spot in a grain silo is very important. They realize a small silo, filled with barley, to see the capability of thermal imaging to detect a hot spot inside the silos. Artificial heat sources were used placed in 9 different locations inside the bulk and setup at 4 temperature levels (30, 40, 50, and 60 °C) in each location. The infrared thermocamera was placed on the top of the silos (the outer surface) and a hot spot was choosen. If the wind had a velocity of 1, 1.5, 2 m/s it was impossible to detect the hot spot. The same situation happened when the ambient temperature was 1°C and silo wall temperature was –8 °C. Hot spot was detected from the thermal images when was located 0.3 m from the silo wall and 0.3 m below the grain surface, respectively. They reported that is not possible to use only the thermal imaging to monitor the grain temperature on the silo.

Manickavasagan, et al. has developed in 2008 an infrared thermal imaging system to identify eight western Canadian wheat classes. The wheat samples were heated by a plate maintained at 90 °C, and the surface of the grain bulk were imaged. The samples were imaged before heating, after heating for 180 s and after cooling for 30 s using an infrared thermocamera.

This research showed the potential and accuracy of thermal imaging for classification of wheat cultivars which are difficult to distinguish by visual inspection, and may have potential to develop classification methods for varieties and grain. Other investigation is required to study the performance of this system

for wheat from different crop years, samples mixed with defects (drought stressed and other defects), and samples of varying kernel sizes and quality (such as protein) within a class (Manickavasagan, & al., 2008).

More and more researchers study this field to evaluate the maturity state of fruits and vegetables. The first ones were Danno, Miyazato and Ishiguro on 1980. When the organic products (fruit and vegetables) generate heat in the metabolic processes, the IR thermocamera can detect this temperature change on the surface. The fruits and vegetables analyzed were: Japanese Persimmon, Japonese Pear and tomato. They applied the same techniques as the ones used for grading apple for bruise and to discriminate of hatching eggs during the incubation period. The grade of maturity was divided in three categories: immaturity, maturity and over-ripe depending on their colour, firmness and sugar content. The samples were kept in two thermo-regulated rooms at 30 degrees and 5 degrees, respectively. The changes in the surface temperature and the grade of maturity of samples were investigated and also the relationship between the surface temperature and the grade of maturity of the samples.

Varith et Al. (2003) have studied the use of infrared thermography to detect bruises on apples stored at 3°C that were heated at 26°C with hot air. It's possible to detect apple bruise with thermal imaging because differences in temperature between sound tissues and bruised were detected, depending on their thermal properties. To detect the bruised apples, four thermal properties were associated in heat transfer: thermal diffusivity (α), thermal conductivity (k), specific heat (Cp), and thermal emissivity (ε). Stroshine, 1998 related that the damaged cells release water into tissue air spaces, which may increase the thermal conductivity. Mohsenin (1996) demonstrated that the moisture in old bruises

migrates out of damaged tissue, leaving a brown bruise, reducing bruise mass, density, specific heat and possibly thermal conductivity.

They reported the difference from the sound tissue within 30-180 s was at least 1-2°C in thermal images, and the asymmetries differences were possibly due to the differences in thermal diffusivity. They accept that these techniques provide good information about automatic bruise sorting and maybe some information to understand better the bruise tissue of the apples.

Other researches on apples were conducted by Veraverbeke et al. (2006) to monitor the cooling rate and surface temperature in relation to the surface quality and wax layer structure before and during storage. The first step in this research was to determine the emissivity, 0.96, for two different cultivars Jonagored and Elshof. After that they recorded the cooling from 20 °C to 12 °C they showed that the Elshof apples had a faster cooling rate and lower temperature than Jonagored apples, which may be related to differences in wax structure between these cultivars. The changes in wax structure occurred during storage were not detected using thermographic imaging.

The most recent researches to detect early bruise in apples resulted in a system made by Baranowski et al. (2012) that incorporates the hyperspectral imaging and infrared thermal imaging. Hyperspectral image analysis was performed by application of principal components analysis (PCA) and minimum noise fraction (MNF). Thermal imaging (3000-5000nm) is useful for bruise recognition when an active approach (lock-in or pulsed-phase) is applied.

The created models of supervised classification based on VNIR, SWIR and MWIR ranges show that best prediction efficiency for both distinguishing bruised and sound tissues as well as for detecting bruises of various depths is

obtained for models using these three ranges together; the conclusion is that it is recommended to include MWIR range into sorting systems.

Thermal imaging was first used by Van Linden, Vereycken, Bravo, Ramon, and De Baerdemaeker (2003) to detect tomato bruise.

They compared three temperature treatments with respect to bruise detection. The analysis process contained the following steps: cooling the tomatoes for 90 minutes at 1°C then warming them up in an oven at 70°C for 1 or 2 min. and shortly warming them up by means of microwaves during 7 or 15 s. The most significant differences between bruised and intact tissue were after a 15s treatment by means of microwaves, observing cold circular spots of bruises on thermal images of the tomato surface.

This experiment provides a good method for automatic bruise detection of tomatoes.

Wang et al. (2006) use the infrared thermocamera to determine the surface temperature distributions of walnut kernels during radio frequency (RT) treatment protocols to control insect pests in in-shell walnuts. A pilot system was used to determine the effect of process parameters on walnut temperature distribution. Temperatures of vertically oriented walnuts were 7.4 °C higher than those of horizontally oriented walnuts. They report that the open shell walnuts are heated much faster in RF systems than closed shell walnuts after 1.5 minutes of bleaching. When they mix twice the walnuts during 3 min. of RF treatment improved the heating uniformity of final walnut temperatures. This experimental provide very useful information for designing an industrial scale quarantine security process against insect pest in walnuts as an alternative to chemical fumigation.

Fito et al. (2004) reported the use of infrared thermocamera to control citrus surface drying by image analysis. Drying citrus surface is an important operation in a fresh fruit processing plant, but air temperature is very difficult to control. In industry, excessive air temperature is usually used or the fruit are left long time in the drier, decreasing the fresh fruit shelf life and also causing a loss of sensorial quality.

They tested a new system using infrared technique to control the surface drying time by image analysis of the fruit surface temperature distribution. The oranges from Valencia Late variety were washed with water or covered with wax and were dried at 20, 25 and 35°C at different air velocity 1, 1.5, respectively 2 m/s. The fruit emissivity was measured by tempering the fruits at 20 degrees and the value of that it's 0.95. The surface temperature during the drying process was measured with an AGEMA 470 the lowest surface temperature of the fruit was assumed to be the wet bulb temperature.

They considered that the drying time could be established when the temperature at any point of the citrus surface exceeded this value.

They created also an empirical model to correlate drying times with air conditions, and these parameters can be used in industrial control systems for citrus surface driers. Image analysis of infrared thermography has a good applicability in food industry to determine the moment when surface drying ends and the peel drying begins. This nondestructive technique offers a real possibility to control better the heat consumption and fruit quality.

Albert et al. in 2011 reported the study "A film of alginate plus salt as an edible susceptor in microwaveable food". The research was made using infrared thermal imaging. As they said, cooking or warming battered and breaded foods in

a microwave oven results in a lack of crunchiness due the way microwaves heat foods. They tried to solve this problem with a film of alginate gel with high salt concentration between substrate and batter used as an edible susceptor.

They prepared chicken nuggets sample with alginate coating set in a calcium chloride (3%) plus sodium chloride (10%, 20%, and 30%) solution bath.

The prefried nuggets were cooked in a microwave oven at different cooking times were used: 15, 20, 25, 30, 35, 40, 45, 50, 55 and 60 s. A thermal camera was used to observe how heat was distributed once this new film of alginate plus salt was incorporated. They took out the nugget sample from the microwave after each preselected time, sectioning it perpendicularly through the center immediately after, separating the two halves, and thermographing the two exposed cross sections. They set the emissivity of the nuggets at 0.920. The temperature distribution was registered from each sample's thermogram. They observed that the alginate films produced more even heating patterns of the nuggets and shorter cooking times and it can be concluded that this technique has given a useful tool to study the edible susceptor performance.

Lahiri et al. (2012) applied infrared thermography in the microbiology field research. They studied the detection of some pathogenic gram negative bacteria (Vibrio cholerae, Vibrio mimicus, Proteus mirabilis, Pseudomonas aeruginos) using this technique. The conventional methods of enumerating bacteria require labor-intensive and are usually time consuming. During the metabolic activities all the organisms generate heat, measuring this energy is a viable tool to detect and quantify bacteria.

They also observed that, the energy content; defined as the ratio of heat generated by bacterial metabolic activities to the heat lost from the liquid medium

to the surrounding, vary linearly with the bacterial concentration in all the four pathogenic bacteria (Lahiri et al., 2012).

This research shows that infrared thermography could be employed as a real-time, non-contact alternative for quantification of clinically significant pathogens. More studies are required to test the universality of this new approach to be applied for a wide range of pathogens.

I.3. References

Albert, A., Salvador, A., Fiszman, S.M. (2011). A film of alginate plus salt as an edible susceptor in microwaveable food. *Food Hydrocolloids, 27*, 421 - 426

Baranowski, P., Mazurek, W., Wozniak,J., Majewska,U. (2012). Detection of early bruises in apples using hyperspectral data and thermal imaging. *Journal of Food Engineering 110*, 345–355.

Burnay, S.G, Williams, T. L. & Jones, C. H. (1988) Applications of Thermal Imaging, *Bristol: Hilger*

Castro, L. M. & Gavarrete, E. (2000). Competitividad en Centroamérica 1999. CEN 1405, Centro Latinoamericano para la competitividad y el desarrollo sostenible. *CLACDS/INCAE*, San José.

Carino, N.J. (1994). Concrete Technology: Past, Present and Future. Nondestructive Testing of Concrete: History and Challenges, *American Concrete Institute (ACI SP-144)*, 623-678.

Chrzanowski, K., & Rogalski, A. (2006). Infrared devices and techniques. *Handbook of Optoelectronics (Two-Volume Set) Edited by Robert G . W . Brown and John P Dakin Taylor & Francis*, 653–692

Costa, L. N., Stelletta, C., Cannizzo, C., Gianesella, M., Lo Fiego, D. P., & Morgante, M. (2007). The use of thermography on the slaughter-line for the assessment of pork and raw ham quality. *Italian Journal of Animal Science, 6*, 704 - 706.

Danno, A., Miyazato, M., & Ishiguro, E. (1980). Quality evaluation of agricultural products by infrared imaging method. III. Maturity evaluation of fruits and vegetables. *Memoirs of the Faculty of Agriculture Kagoshima University, 16*, 157 - 164.

Du, C. J., & Sun, D. W. (2004). Recent developments in the applications of image processing techniques for food quality evaluations. *Trends in Food Science & Technology*, *15*, 230 - 249.

Fito, P. J., Ortola´, M. D., De los Reyes, R., Fito, P., & De los Reyes, E. (2004). Control of citrus surface drying by image analysis of infrared thermography. *Journal of Food Engineering, 61(3),* 287 - 290.

Flir (2010). The ultimate infrared handbook for R&D professionals.

Foster, A. M., Ketteringham, L. P., Purnell, G. L., Kondjoyan, A., Havet, M., & Evans, J. A. (2006). New apparatus to provide repeatable surface temperatureetime treatments on inoculated food samples. *Journal of Food Engineering*, 76, 19 - 26.

Foster, A. M., Ketteringham, L. P., Swain, M. J., Kondjoyan, A., Havet, M., Rouaud, O. et al. (2006). Design and development of apparatus to provide repeatable surface temperature etime treatments on inoculated food samples. *Journal of Food Engineering*, *76*, 7 - 18.

Fuller, M. P. & Wisniewski, M. (1998). The use of infrared thermal imaging in the study of ice nucleation and freezing of plants. *Journal of Thermal Biology, 23*, 81 - 89.

Giaime Ginesu, Daniele D. Giusto, Volker Märgner, & Peter Meinlschmidt (2004). Detection of Foreign Bodies in Food by Thermal Image Processing, *IEEE Transactions on industrial electronics*, *Vol. 51, no. 2.*

Goedeken, D. L., Tong, C. H., & Lentz, R. R. (1991). Design and calibration of a continuous temperature measurement system in a microwave cavity by infrared imaging. *Journal of Food Processing & Preservation*, *15*, 331 - 337.

Gowen, A. A., Tiwari, B.K., Cullen, P.J., O'Donnell, C.P., McDonnell, K. (2010). Applications of thermal imaging in food quality and safety assessment. *Trends in Food Science & Technology 21*, 190-200

Herschel, W. (1800) Experiments on the refrangibility of the invisible rays of the Sun *Phil. Trans. Roy. Soc.* London 90 284

Ibarra, J. G., Tao, Y., Walker, J., & Griffis, C. (1999). Internal temperature of cooked chicken meat through infrared imaging and time series analysis. *Transactions of ASAE, 42*, 1383 - 1390.

Ibarra, J. G., Tao, Y., & Xin, H. (2000). Combined IR imaging-neural network method for the estimation of internal temperature in cooked chicken meat, *Society of Photo-Optical Instrumentation Engineers 39*, 3032 - 3038

Kaiser, P. K. (1996). The joy of visual perception. http://www.yorku.ca/eye/spectru.htm Accessed 15 Jan 2011.

Kolzer, J., Oesterschulze, E., Deboy, G. (1996). Thermal imaging and measurement techniques for electronic materials and devices, *Microelectronic Engineering, 31*, 251–270

Lahiri, B.B., Divya, M.P., Bagavathiappan, S., Thomas, S., Philip, J. (2012). Detection of pathogenic gram negative bacteria using infrared thermography, *Infrared Physics & Technology 55*, 485 - 490

Luong, M.P. (2007). Introducing infrared thermography in soil dynamics. *Infrared Physics & Technology*, 306-311

Lloyd, J. M. (1975), Thermal Imaging Systems

Maierhofer, Ch., Arndt, R., Röllig,M., Rieck, C., Walther, A., Scheel & H., Hillemeier, B. (2006). Application of impulse-thermography for non-destructive assessment of concrete structures. *Cement & Concrete Composites 28*, 393-401

Maldague, X., Galmiche, F., & Ziadi, A. (2002). Advances in pulsed phase thermography. *Infrared Physics & Technology, 43*, 175 -181.

Maldague, X., (2002), Introduction to NDT by Active Infrared Thermography, *Materials Evaluation, 6*, 1060 -1073,

Manickavasagan, A., Jayas, D.S., White, N.D.G., & Paliwal, J. (2008). Wheat class identification using thermal imaging. *Food and Bioprocess Technology 3*, 450–460

Manickavasagan, A., Jayas, D. S., White, N. D. G., & Jian, F. (2006). Thermal imaging of a stored grain silo to detect a hot spot. *Applied Engineering in Agriculture, 22*(6), 891 - 897.

Mayer F, Feldmann, O. (2001) Optical Measurements (Techniques and Applications), *2nd edn. Springer-Verlag*,

Meola, C., Carlomagno, G.M. (2004). Recent advances in the use of infrared thermography, *Measurement Science and Technology 15*, 27–58.

Mohsenin, N. N. (1996). Mechanical damage. *Physical Properties of Plant and Animal Materials*, 481 – 615. Canada: Gordon and Breach Publishers.

Mori, M., Novak, L., Sekavčnik, M., Kuštrin, I. (2008). Application of IR thermography as a measuring method to study heat transfer on rotating surface - *Forschung im Ingenieurwesen, Springer-Verlag*.

Moss, C.E., Ellis R.J., Murray W.E., Parr, W.H., (1988). Nonionizing radiation protection. Infrared radiation. *WHO Reg Publ Eur* Ser. 85-115.

Nott, K. P., & Hall, L. D. (1999). Advances in temperature validation of foods. *Trends in Food Science & Technology, 10*, 366 - 374.

Omar, M., Hassan M. I., Saito K., and Alloo, R. (2005). IR self-referencing thermography for detection of in-depth defects, *Infrared Phys. Technology*, *vol. 46 (4)*, 283 - 289.

Petersen J . K . (2012). Handbook of Surveillance Technologies, Third Edition *CRC Press*.

Rao, D. S. Prakash (2008), Infrared thermography and its applications in civil engineering, *Indian Concrete Journal*

Rogalski, A. (2000). Infrared Detectors. *Gordon and Breach Science* Amsterdam: Gordon and Breach)

Ross, W. (1994) Introduction to Radiometry and Photometry, Boston: Artech

Sakagami, T., Kubo, S. (2002). Applications of pulse heating thermography and lock-in thermography to quantitative nondestructive evaluations. *Infrared Physics & Technology 43*, 211–218

Shepard, S. M., Ahmed, T., & Lhota, J. R. (2004). Experimental considerations in vibrothermography. Experimental considerations in vibrothermography. *Proceedings of SPIE, 5405*, 332.

Stroshine, R. (1998). Thermal properties and moisture diffusivity. *Physical Properties of Agricultural Materials and Food Products*. 217 –238. Purdue University, West Lafayette, IN.

Vadivambal, R., & Jayas, D. S., (2010). Applications of thermal imaging in agriculture and food industry—a review. *Food and Bioprocess Technology*.

Van Linden, V., Vereycken, R., Bravo, C., Ramon, H., & De Baerdemaeker, J. (2003). Detection technique for tomato bruise damage by thermal imaging. *Acta Horticulturae (ISHS), 599,* 389 - 394.

Varith, J., Hyde, G. M., Baritelle, A. L., Fellman, J. K., & Sattabongkot, T. (2003). Non-contact bruise detection in apples by thermal imaging. *Innovative Food Science and Emerging Technologies, 4,* 211 - 218.

Vavilov, V. P., (1992) Thermal non-destructive testing: short history and state-of-art *Proc. QIRT 92 (Paris)* ed D Balageas, G Busse and G M Carlomagno (Paris: EETI editions), 179–93

Veraverbeke, E. A., Verboven, P., Lammertyn, J., Cronje, P., De Baerdemaeker, J., & Nicolai, B. M. (2006). Thermographic surface quality evaluation of apple. *Journal of FoodEngineering, 77,* 162 - 168.

Wang, S., Tang, J., Sun, T., Mitcham, E. J., Koral, T., & Birla, S. L. (2006). Considerations in design of commercial radio frequency treatments for postharvest pest control in in-shell walnuts. *Journal of Food Engineering, 77,* 304 - 312.

Weil GJ. (1992) Non-destructive testing of bridge, highway and airport pavements. *No Trenches in Town Proceedings of International Conference*, Paris, France; 243–6.

Workmaste, B. A., Palta, J. P., & Wisniewski, M. (1999). Ice nucleation and propagation in cranberry uprights and fruit using infrared video thermografy. *Journal of the American Society for Horticultural Science*, USA, 124

Zayicek, P., (2002) Infrared Thermography Guide (Revision 3), *EPRI, Palo Alto*.

II. APPLICATION OF INFRARED THERMOGRAPHY IN THE FOOD INDUSTRY

II.1 Experimental validation of a numerical model for hot air treatment of eggs in natural convection conditions and with hot-air jet with FLIR- IR thermocamera

II.1.1 Introduction

It is well known that eggs are a very important nutritive product, but also that there are certain problems that can derive from the consumption of eggs with pathogenic bacteria. The main goal and all effort should concentrate to inactivate these microorganisms in order to provide consumers safe and healthy products. In this direction, the use of all new technology is required and provided to food operators so they can have better control methods during the production flux. The most efficient known decontamination method for egg shells was reported by Standelman (1996) and Hou (1996) with no significant differences regarding the denaturation of protein between the fresh and pasteurized eggs in the oven. At the same time, they reported a reduction of the Salmonella Enteritidis by 5 log 10 loads on yolk of eggs, after the treatment in the oven at 55 °C for 180 min.

On the other hand, James et al. (2002) reported significant reduction in Salmonella numbers without damaging the egg content, with heat treatments using a hot-air gun. The aim of this research was to validate the numerical model for hot air treatment of eggs in natural convection condition and with hot-air jet, using the experimental data obtained with an infrared thermocamera.

The models realized by Cevoli et al. (2010) and Fabbri et al. (2010) to simulate a hot-air treatment of the egg shell was compared with experimental data on the shell eggs using the thermocouples.

For the first validation, the treatment with hot air, in natural convection conditions, the calculated temperature was compared with experimental data on the egg shell obtained using the infrared thermocamera.

For the second validation, the treatment with hot-air jet using high temperatures (300-500°C) to decontaminate the shell egg, the calculated temperatures, were compared with experimental data observed. The potential of treatments using high temperature was tested in the past by James et al. (2001) and Pasquali et al. (2009). James et al. (2001) heat the eggs at 500 degrees for 8 seconds, but they don't make any microbiological test. Instead, Pasquali et al. (2009) used the prototype realized in the past to do a decontamination of shell eggs using a hot air jet (600°C, two shots) in one side with an interval of 30 seconds and with an cold air jet for 30 seconds (1 shot) on the opposite side of the egg. They investigated 380 eggs load on S. Enteritidis, during 24 days of storage at 20 °C. Half of them were head treated, and half not. The hot air treatment reduces the bacterial S. Enteritidis load on eggshells up to 1.9 log and they conclude that the pasteurization using the hot air are useful for decontamination of table eggs.

This research is important to determine the distribution of temperature on the egg shell surface to have a good control during the decontamination of eggs shell and not to affect the quality of content of the eggs.

II.1.2 The eggs

The European Parliament and the European Council defined by Regulation (EC) No 853 /2004, the "Eggs" means eggs in shell – other than broken, incubated or cooked eggs – that are produced by farmed birds and are fit for direct human consumption or for the preparation of egg products. When shell is removed, we can talk about the “egg products”. In the food industry the most used egg products are liquid, frozen and dried, products that are safe for consumers.

The eggs are one of the highest quality sources of important nutrients and they are also easily digested. According with FAO Stats, the level of global production is about 1.182 billion eggs per year in 2011 or 64 million tons. The sector of poultry and eggs production was the most dynamic sector in the last 10 years, which was reflected in growing demand for these products. According with FAO, 2010, in the developing countries the consumer preferences are changing, increasing the protein demand, especially for low-priced foods such as eggs, gradual shift in consumption from pork to poultry. The easy way to cook the eggs and poultry meat changed the lifestyle of many people and this will continue in the future.

Poultry meat and eggs are a very important source of protein and can be eaten by all healthy consumers. The eggs are 88.5% edible and are composed of three main parts: shell, egg white, egg yolk. The shell of an egg is a porous part that allows the oxygen to enter for the chick but bacteria and different odours can also enter, and water and CO2 can escape.

The shell egg is usually strong and protects the egg against bacteria. The older birds produce eggs with shells less strong and the colour varies to the breed.

The egg white has 2 layers, one near to the shell and another near to the yolk (FAO, 2010). Over the 60% of the world's eggs are produced in industrial systems and the biggest producers are China, United States, India, Mexico.

Eggs are classified in Europe as follows : small size (between 42g and 53g), medium size (53-63 g), large (63-73 g), very large (73 g and over) .

The eggs have a high nutritional content: the white part contains 10.5% proteins, 88.5% water, riboflavin and more vitamins from B group and on the other hand the yolk part has more nutrients, 16.5% protein, 33% fat, 50% water, vitamins A, E, K, D, some minerals, emulsifier (lecithin) (FAO, 2010).

In food preparations the eggs are used for: thickening - because of the coagulation of the egg proteins; emulsifying – to make mayonnaise, cakes because eggs contain lecithin; binding – ingredients for rissoles, croquettes; coating – they form the protective layer during frying foods and prevent overcooking; glazing – used to produce a golden brown shiny glaze during baking the pastries and bread.

Salmonella

One of the most problematic things for using eggs is the contamination with bacteria such as Salmonella enterica serotype Enteritidis, existing in the hen's ovary or oviduct before the shell forms around the white part and yolk. S. Enteritidis is the serovar which causes more than 60% of human infections with Salmonella in the European Union (EFSA, 2009). Salmonella belongs to the Enterobacteriaceae family and is a mesophilic bacteria, developing at temperatures between 5.2°C and 47°C and optimally between 35°C and 37°C, at pH between 4.5 and 9, with water activity (Aw) greater than 0.93 and appear as

Gram-negative, 0,3 to 1μm wide and 1 to 6 μm microns long (Romane et al. 2012).

The genus Salmonella consists of only two species:

- S. enterica, which is divided into six subspecies: S. enterica subsp, enterica, S. enterica subsp, salamae, S. enterica subsp, arizonae, S. enterica subsp, diarizonae, S. enterica subsp. houtenae, and S. enterica subsp, indica; and
- S. bongori (Popoff & all., 1998)

A total of 2501 different Salmonella serotype were identified until 2004, almost all of them causing disease in humans. Other serotypes affect only a few animal species (host-spectrum), like Salmonella Choleraesuis in pigs, Salmonella Dublin in Cattle. When this serotypes cause disease in humans, it is very invasive and can be life-threatening. Usually, these kind of strains cause gastroenteritis, which is often uncomplicated and does not need treatment, but can be severe for people with weakened immunity, like the young and the elderly patients (WHO, 2005). Salmonella Enteriditis and Salmonella Typhimurium are the two most important serotypes for salmonellosis transmitted from animals to humans. S. Enteritidis caused the most recent epidemic, which peaked in humans in 1992 in many European countries. (WHO, 2005). Infection from contaminated food occured for humans when individuals had contact with infected animals, including domestic animals such as dogs or cats.

The contamination can come from faeces when the bacteria pass the pores of the shells of the egg. The most frequently foodborne diseases worldwide are salmonellosis. In the first few minutes, after the oviposition, the eggshell can be more easily penetrated by bacteria according with Miyamoto et al., 1998 and

Padron, 1990. After the oviposition, the bacteria can penetrate the eggshell and membranes more easy because the egg comes to temperatures cooler than the chicken body temperature (42 °C), perhaps creating a negative pressure (Board, 1966). The ideal conditions for penetration of the egg shell by bacteria was hypothesized by Berrang et al., 1999, and can be the moment a warm egg encounters a moist and cool environment.

According with EFSA (2012) the salmonellosis is the second most frequently reported zoonosis in UE and continues to decrease. Unfortunately we have reported data about the economic cost of the disease only for few countries.

According with World Health Organization (2005) in the United States of America an estimated 1.4 million non-typhoidal Salmonella infections, resulting in 168 000 visits to physicians, 15 000 hospitalizations and 580 deaths annually, with a cost estimates per case of humane salmonellosis range from 40 to 4,6 million US$, respectively for uncomplicated cases to cases ending with hospitalization and death. It's estimated a total cost associated with Salmonella at US$ 3 billion annually in the United States of America (WHO, 2005). On the other hand, in Denmark, the annual estimated cost of foodborne salmonellosis is US% 15, 5 million in 2001, representing 0.009% of Gross domestic product (GDP).

The symptoms of human salmonellosis are usually characterized by acute onset of fever, abdominal pain, diarrhoea, nausea and sometimes vomiting. In some cases, particularly in the very young and in the elderly, the associated dehydration can become severe and life-threatening. Serious complications occur in a small proportion of cases. In such cases, as well as in cases where Salmonella

causes bloodstream infection, effective antimicrobials are essential drugs for treatment (WHO, 2005).

The optimal treatments of salmonellosis for adults are the antimicrobials from the fluoroquinolones group. They have a good oral absorption, well tolerated and are relatively cheap. Instead for the children with serious infections the most frequently used treatment is cephalosporins (injection). As an alternative, others drugs like chloramphenicol, ampicillin, amoxicillin and trimethoprim-sulfamethoxazole can be used.

Starting 2012, all the European states were required to implement the CE Directive 74/1999 concerning obeying the minimum standards for poultry farms, replacing traditional systems with battery farming systems on the ground or battery that provides better condition and more space.

Normally these new systems increase the risk of contamination of eggs with various microorganisms, mainly with Salmonella Enteritidis that can harm the human health. In Europe is not allowed to wash the eggs with hot water, like in USA. In this case we have to find other methods to decontaminate the egg shell. In the past only few studies have been published about the use of hot air to decontaminate the shell of eggs. In the 1996, Hou et al. observe that after heating at 55°C in a hot air oven for 180 min gave a 5 log 10 reductions of Salmonella Enteritidis. Other researches like James et al (2002) verified the applicability of treatment in a stream of hot air for the pasteurization of the egg surface, but they did not assess the potential of the technique to decontaminate the eggs. In 2010, Manfreda et al. (2010) reported good results about the treatments with hot air for the surface decontamination of table eggs experimentally contaminated by salmonella enterica serovar Enteritidis. They used a treatment with two shots of 8

s at 600°C, with an interval of 30s of cold air. The results show that this kind of treatments can reduce the S. Enteritidis load on eggshells of up to 1.9 $\log_{10}$.

The results for egg shell obtained from the experiment with an FLIR infrared thermocamera were compared with data from the numerical model for hot air treatments obtained in the past by Fabbri et al. (2010).

II.1.3. Material and methods

A. Determination of egg emissivity

The current study required the experimental measurement of temperature of eggs shell during the hot-air treatments using FLIR-IR thermocamera. This experiment can be very useful to obtain important data with a nondestructive method. In order to determine the temperature of the egg shell we have to know the coefficient of emissivity of the egg shell. In the literature, unfortunately we don't have too much data about the radiation heat transfer emissivity coefficient, because these techniques are recently used in the field of food industry. This is an obstacle for the companies who want to use the infrared thermography in the food processing because they will spend more time to determine this coefficient.

All the objects have a different emissivity that depends on the nature of the emitting object, temperature and other parameters. These parameters are the most important when an infrared thermocamera is used, because this is a measure of how much radiation is emitted from an object, compared to that from a perfect blackbody of the same temperature (FLIR, 2010).

To determine the emissivity we use the equation II.1:

$$W = \varepsilon\sigma T^4 \ [\text{Watt/m}^2] \ \text{(II.1.)}$$

where W is the total power emitted at 7.5 - 13.0 μm in Wm^{-2}, ε is the emissivity of the target (1 for the perfect body), σ is the Stefan-Boltzmann's constant (5.67051 x 10^{-8} $Wm^{-2}K^{-4}$), T is the temperature of the target object in Kelvin degree.

The radiance entering a thermographic camera originates from three sources (Lamprecht et al., 2002): (i) the observed object itself; (ii) other objects reflected on the target's surface, and; (iii) an atmospheric contribution.

The equation II.2 can also be used to determine the emissivity:

$$W = \sigma(\varepsilon T_{egg}^4 + (1-\varepsilon)T_{amb}^4 - T_{Pyr}^4) \text{ [Watt/m}^2\text{]} \quad \text{(II.2)}$$

where W is the total power emitted at 7.5 - 13.0 μm in Wm^{-2}, ε is the emissivity of the target (1 for the perfect body), σ is the Stefan-Boltzmann's constant (5.67051 x 10-8 Wm-2K-4), T_{egg} is the temperature of the target object, egg in our case, in Kelvin degree, T_{amb} is the temperature of background radiation, T_{pyr} is the temperature of the device/air. I used the standard method for measuring the emissivity (ASTM, 2003) using a surface-modifying materials that can change the heat transfer properties and temperature of the specimen.

The infrared energy emitted by a target object, eggs in our case, is related to the temperature of the object by means of its emissivity. Usually, emissivity of the non-metals tends to be high, and decreases with temperature. The measurement of absolute temperature requires the knowledge of the emissivity of the material, a seldom available parameter for food product, or the calibration of the thermocamera using reference materials (Al foil) having known emissivity.

A thermocamera FLIR model A325 was used to determine the emissivity of egg. The model used works in the spectral range 7.5 to 13.0 μm, has a pixel resolution of 320×240, with an operating temperature range between -15°C to +50°C. The most important advantage of this method is that we don't need a physical contact with the eggs to find the emissivity and temperature.

The eggs to be measured were placed in a thermostatic cooling room at a constant temperature of 20°C for 24 hours, and half of the eggs were covered with

aluminum foil with known emissivity of 0.04. Were used 15 different eggs during different days. The infrared thermocamera was fixed inside of the cooling room and a schematic representation of this the setup is shown in the *figure 5*. This allowed having a homogeneous temperature of the target object – egg, with a clear difference in radiation between background and the egg.

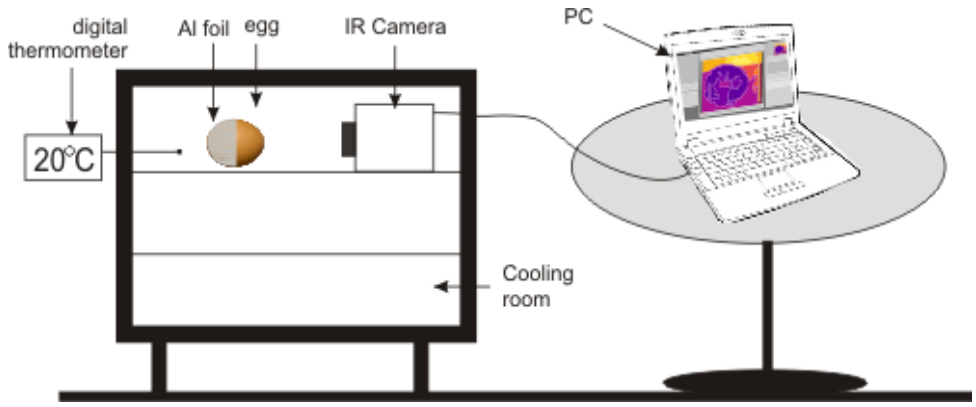

Figure 5 Infrared Thermocamera FLIR A325 setup

The infrared camera was connected at one PC and the images were recorded using the FLIR Research and Development Software to obtain a thermogram. An automatic calibration of the thermocamera for the thermostatic room temperature and air humidity was provided. The thermostatic room was without light inside to obtain a minimal reflection from the background. For this experiment, the reference material aluminum foil with known emissivity (ε=0.04) was used. The emissivity of the camera was set to that of the known material and we can see that we have the same temperature like in the cooling room.

After 24 hours at constant temperature, the egg arrives at equilibrium and the measurements were made to determine the emissivity of egg. We set the instrument emissivity control for the aluminium coated area of the egg, and note

the temperature given by the instrument. Afterwards the temperatures next to this spot (*fig. 6*), on the uncoated area were noted, and the emissivity set was adjusted until we obtained the same temperature like in the above case.

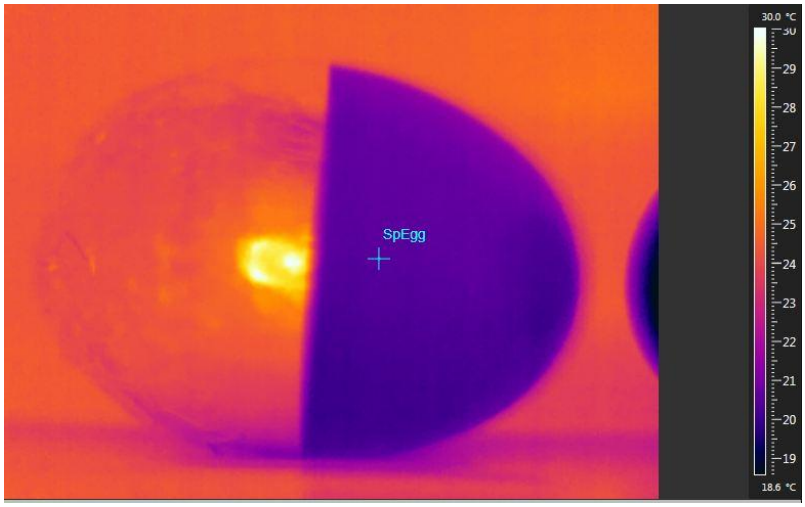

Figure 6 Egg temperature measured with Infrared Thermocamera FLIR A325

We obtained this way the effective emissivity of the shell of egg. The average of egg emissivity over the samples was 0.95 with a standard deviation of 0.01. The egg coefficient of emissivity is very important for the future measurements made with infrared thermocamera to have a real temperature of the shell of egg during the heat treatments.

B. Experimental validation of a numerical model for hot air treatment of egg surface decontamination, in natural convection conditions using an infrared thermocamera

The numerical model realized in the past by model Cevoli et al. (2010) using the experience data about albumen coagulation limit condition reported in

the past by Hou (1996) was validated using an infrared thermocamera. This numerical model was realized using a computational fluid dynamic tool (CFD) based on the Finite Element Technique (Comsol Multiphysics 3.5a, COMSOL Inc., Burlington, MA, USA) and describes the interaction between hot air and the eggs.

The control of heating eggs in the oven was realized using the infrared technique, and we can determine exactly the moment when the shell egg arrives at 55 degree avoiding internal degradation of eggs.

The tested treatments were realized in an oven (MOD 2100, F.lli Galli, Milan, Italy). All the eggs, 10 samples, were tempered at 25ºC before starting the experiment. A wall from extruded polystyrene (Thermo 33 extruded, 50 mm) was placed between the oven heating area and the metallic door like we can see in the *figure 7*, to avoid errors during the thermal process and imaging. The characteristic of this material ensures a good isolation during the short time of opening the metallic door. A perfect window was created for the Flir A 325 dimensions, to capture the thermal imaging.

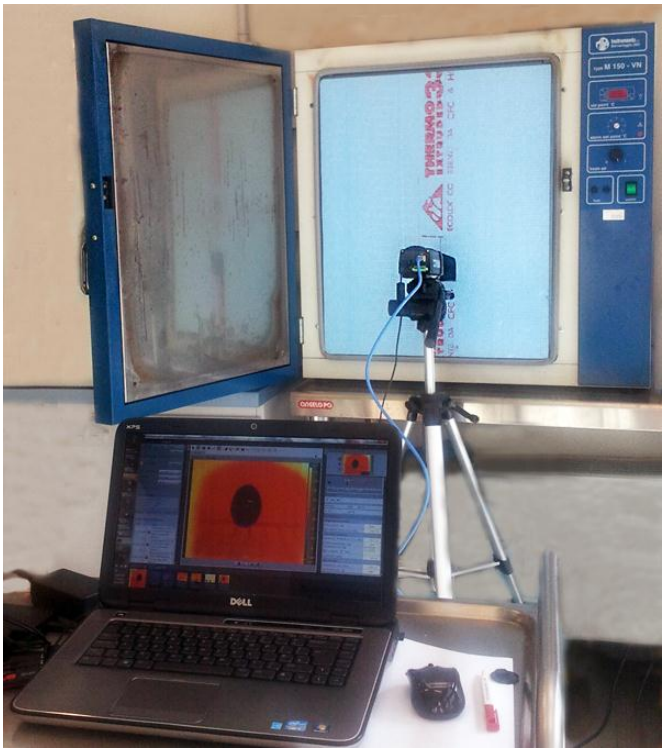

Figure 7 Infrared Thermocamera FLIR A325 setup for measurements in the oven

The treatments were performed in the oven at an air temperature of 55°C for 50, 100, 150 and 200 minutes like in the experience of Hou (1996) and Cevoli et al. (2010). Using this temperature we can have the condition for a high decontamination of eggs and also we respect the albumen coagulation limit conditions. The temperatures were measured during the heating using the infrared thermocamera FLIR A 325 and also an thermocouples (Thermometer model HIBOK 14). The calculated time-temperature curves from the model were than compared with the observed data obtained during these measurements.

C. Experimental validation of a numerical model for hot air treatment of egg surface decontamination with hot-air jet using an infrared thermal camera

The tests treatments were realized using the prototype used for the validation with thermocouple in the past by Fabbri et al. (2010). For this validation the single egg rotate around its principal axis. Two hot-air jets and one cold jet in opposite side of egg were used to decontaminate the egg surface. We alternated the cold and hot air to arrive at highest temperature on the external shell of the egg in very short time to avoid the internal degradation of eggs. The model realized by Fabbri et al. (2010) to simulate a hot-air treatment of the egg shell was compared with experimental data on the shell eggs using the infrared thermocamera.

A special apparatus was used for the experiments. This was provided with 2 hot air gun (Bosh, model GHG 660 LCD-professional, Robert Bosh SpA, Milano, Italy 2300 W) with different steps of settings of temperature to 660 °C, positioned at 150 mm from the egg, preserving the egg content. Other characteristics of the hot air gun were mentioned in the *table 1*.

Table 1 Characteristics of the hot air gun Bosh, model GHG 660 LCD

Characteristic	**Value**
Rated power input	2300 W
Rated voltage	220-240 V
Temperature at the nozzle outlet (approx.)	50–660 °C
Air flow	250–500 l/min
Temperature-measuring accuracy – at the nozzle outlet – on the display	 ± 5% ± 5%

Display operating temperature	-20…+70 °C
Weight according to EPTA-Procedure 01/2003	1 kg
Length	255 mm
Height	255 mm

The rolling cylinders (wheelbase 35 mm) are moved by a transmission belt, linked to a stepping motor server by an electronic speed regulator (Pasquali et al., 2010). This gun is turned on few minutes before exposing the egg at high temperature (350 °C near by the egg). The cold air comes from a high pressure nozzle using a pipe for compressed air, positioned at 120 mm from the cylinders of rolling egg. The cold air jet has the ambient temperature. The infrared thermocamera was fixed on tripod like in the *figure 8*.

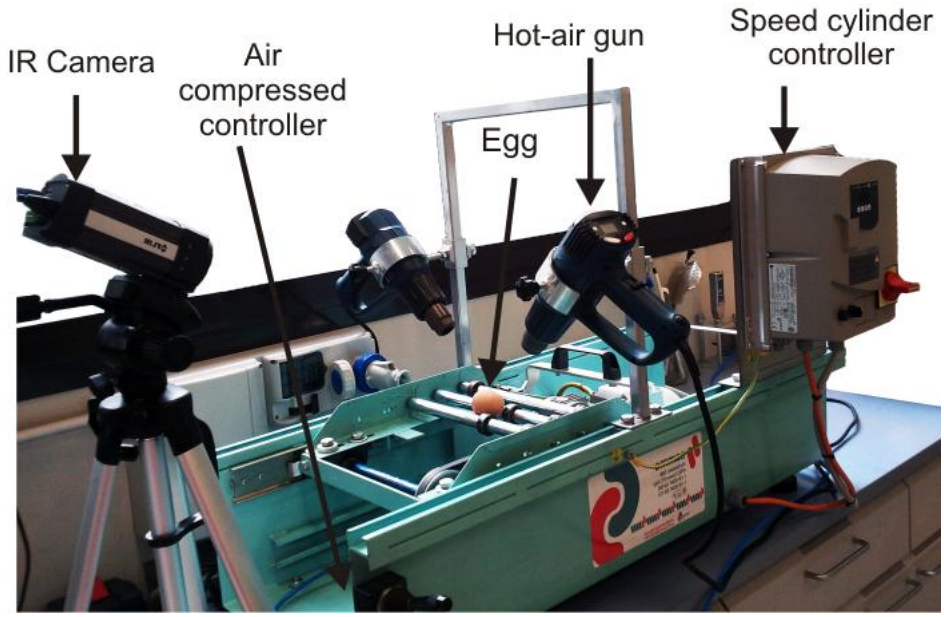

Figure 8 The prototype used for the measurements

Were used the same treatments for the eggs like in the model development and validation describes by Cevoli et al (2010) and Fabbri et. al (2010). For the measurements were used 10 biological eggs for each treatment with an average weight of 65 g. Before starting the experiment, all the eggs were temperate at 30 °C. The parameters for the treatments are detailed in the *table 2*. The speed of the hot air jet was set at 10 ms-1 for all the treatments.

Table 2 Characteristic parameters of the thermal cycles

Treatment	**Duration (s)**	**Cold air speed (m/s)**	**Number of shots**
T1	4	5	1
T2	6	10	1
T3	8	15	1
T4	10	20	1
T5	8+60+8	10	2
T6	8+30+8	15	2
T7	10+30+10	20	2

These treatments reported by Fabbri et all (2010), estimated the external egg shell surface temperature higher than 70 °C and an inner temperature always less than 55 °C to protect the content of the eggs. To measure the air velocity, hot respectively cold, one anemometer was used (Testo AG 445, Ø 10 mm, with telescopic handle, Testo AG, Lenzkirch, Germany). The speed of the egg was set at 0.5 Hz.

The procedure for all the eggs can be described following the steps: the hot air gun were switched on and the highest temperature of 660°C was set near by the exit of hot air, and we have near by the egg position a constant heat temperature for the shell egg at 350 °C. These temperatures were controlled using thermocouples (Thermometer model HIBOK 14). After that, the egg was exposed on the rolling cylinders for heat treatments respecting the parameters of the cycle. For the cycle with one shot the egg was exposed at a hot and cold air flow in the same time for 4,6,8 or 10 seconds. Instead for the cycle with two shots the egg was exposed first at both air flows for 8 or 10 seconds, and after that hot air gun was switched off, and the egg was cooled for 60 or 30 seconds. At the end the simultaneously treatments (heating and cooling in the same time) are repeated for 8 or 10 seconds. During the treatments, every minute the temperature of the egg shell was analyzed using the infrared thermocamera. The parameters of the infrared thermocamera FLIR A 325 are detailed in the *table 3*.

Table 3 Parameters of the infrared thermocamera FLIR, A 325 used during the experiment.

Parameters	**Value**
Emissivity of egg	0.95
Atmosphere temperature	25 °C
Relative humidity	65%
Distance	0.4 m
External optics	25 °C
Temperature range of image	0-350 °C

II.1.4. Results and discussion

For the first validation the simulated temperature of the egg shell was compared with the experimental data obtained by the infrared thermocamera during the heat treatment of the egg in the oven. We analyzed the thermogram (*fig. 9*) data considering the entire surface of the egg using the FLIR ResearchIR Software.

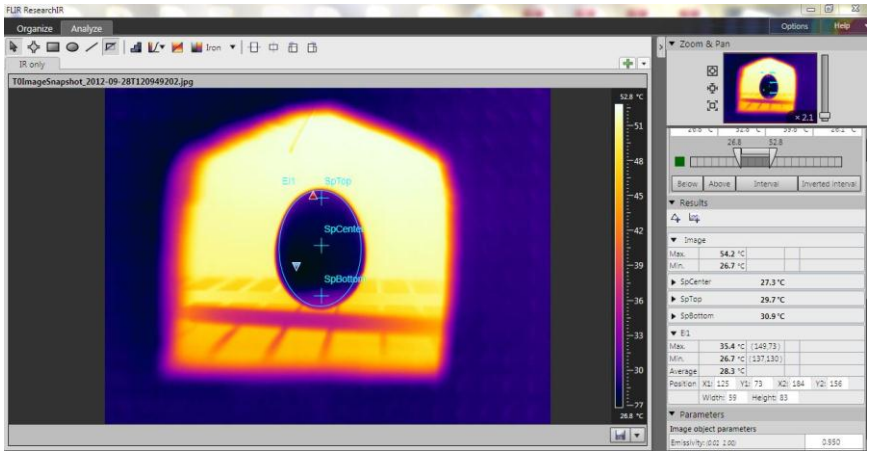

Figure 9 Analysis of the thermographic image for the egg treatment in the oven at 55°C for 200 minutes.

In the *figure 10* the time-temperature curves are shown, minimum, maximum and average temperature of egg heated in the oven for 200 minutes at 55 °C.

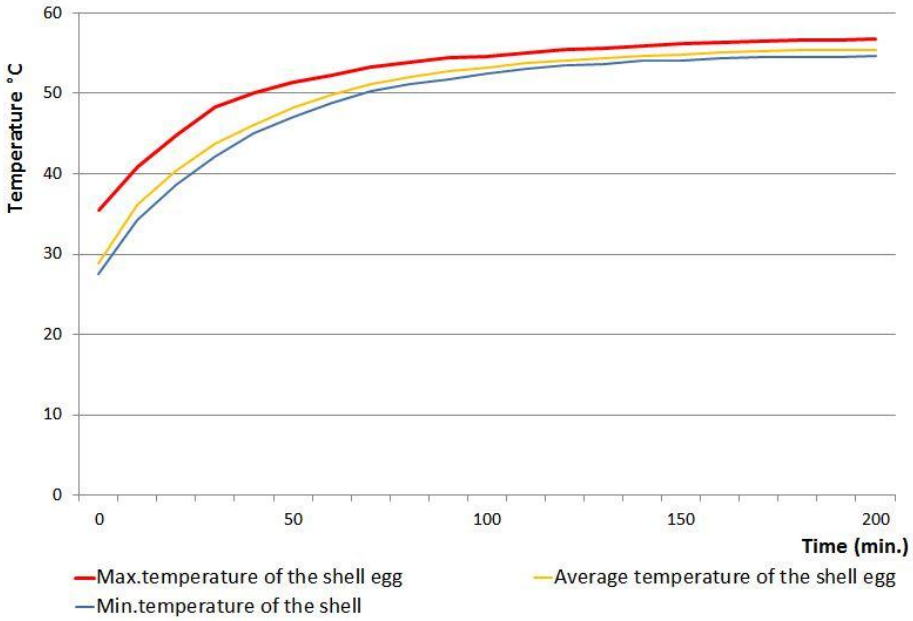

Figure 10 Time-temperature curves observed at the surface of egg shell during the heat treatment in the oven at 55°C, for 200 minutes.

In the following *figure 11*, the simulation data were validated by experimental data obtained with infrared thermocamera.

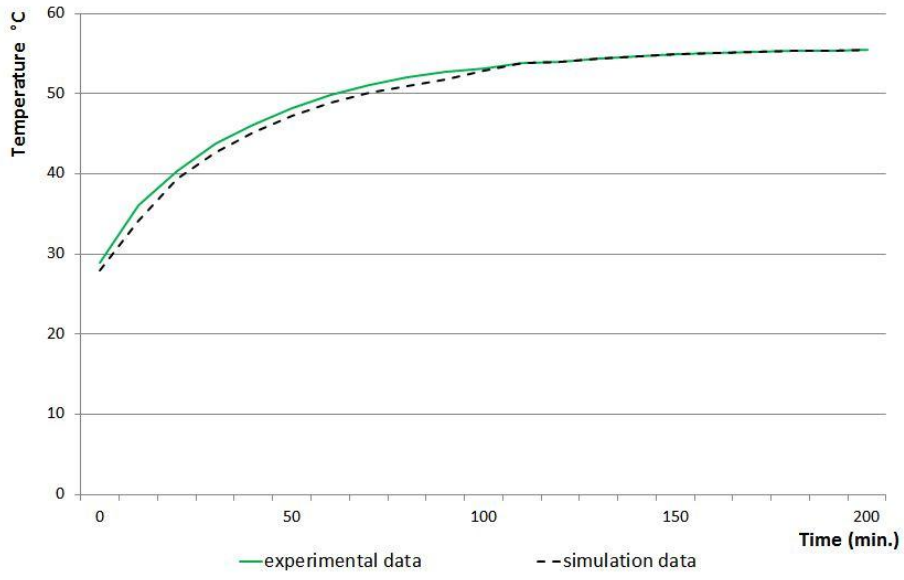

Figure 11 Time-temperature curves of the egg shell measured and calculated

During the head process we can say that the difference between calculated data from the model and measured data is below 2°C.

Second experimental

To have more information and more control about the process of decontamination of eggs using the hot-air gun, the temperatures measured on rotating surface of egg were compared with the simulated temperature profiles of the shell egg. The simulation data were validated by experimental data obtained by infrared thermography.

In the *figure 12, 13, 14, 15, 16, 17, 18* is showed the time-temperature curve calculated and simulated for the equatorial part and over the air cell of the shell egg for each treatment in part. However, the simulated curves and the data from the measurements appear to be in good agreement and we can conclude that the application of infrared thermography to control the egg decontamination using the hot air it's a valid method. The real advantages of this method in this case is that is safe, not-destructive, non-contact, non-invasive and can offer the surface temperatures of the product in real time, with a good accuracy. A great advantage over measurements made with thermocouples is that we can see the entire surface temperature of the product not only in one point.

We can mention also some disadvantages of this method like: it's a new technique used in the food industry, the highest price of the professional cameras, require the training of operators that will perform the thermal measurements, the

resolution of the thermogram are not very high, the ambient reflection of light can influence measurement accuracy.

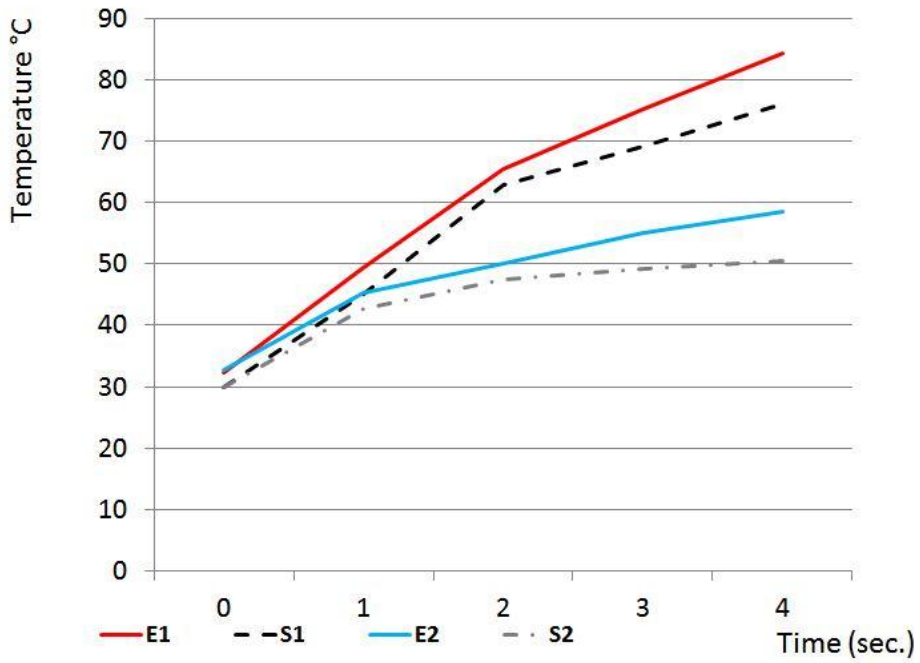

Figure 12 Time-temperature curves of the egg shell measured and calculated for treatment 1. (E1 – measured temperature of shell egg over the air cell, E2 – measured temperature of shell egg on the equatorial part, S1 – calculated temperature of shell egg over the air cell, S2 - calculated temperature of shell egg on the equatorial part)

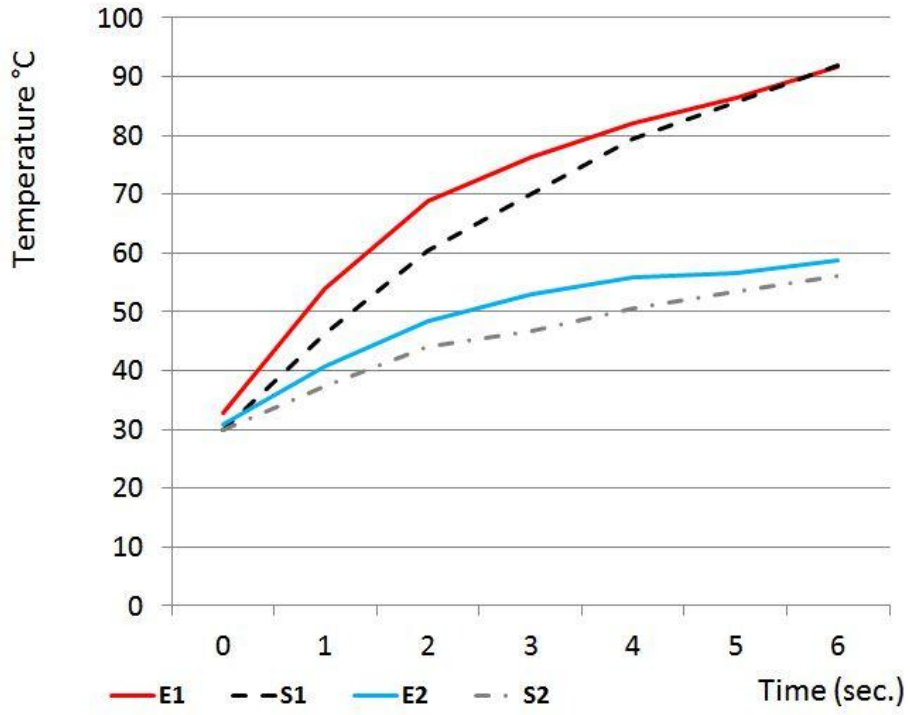

Figure 13 Time-temperature curves of the egg shell measured and calculated for treatment 2. (E1 – measured temperature of shell egg over the air cell, E2 – measured temperature of shell egg on the equatorial part, S1 – calculated temperature of shell egg over the air cell, S2 - calculated temperature of shell egg on the equatorial part)

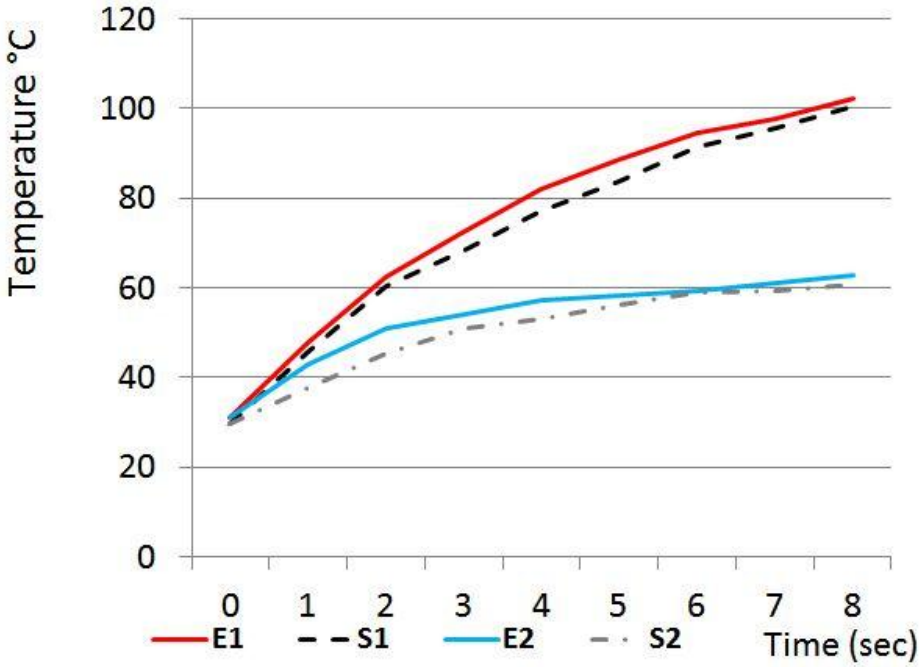

Figure 14 Time-temperature curves of the egg shell measured and calculated for treatment 3. (E1 – measured temperature of shell egg over the air cell, E2 – measured temperature of shell egg on the equatorial part, S1 – calculated temperature of shell egg over the air cell, S2 - calculated temperature of shell egg on the equatorial part)

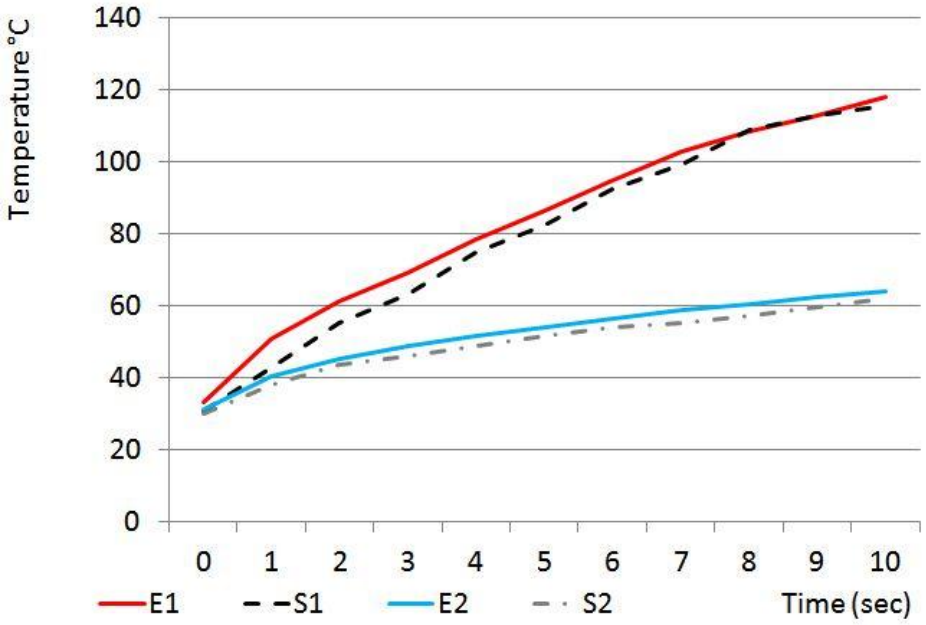

Figure 15 Time-temperature curves of the egg shell measured and calculated for treatment 4. (E1 – measured temperature of shell egg over the air cell, E2 – measured temperature of shell egg on the equatorial part, S1 – calculated temperature of shell egg over the air cell, S2 - calculated temperature of shell egg on the equatorial part)

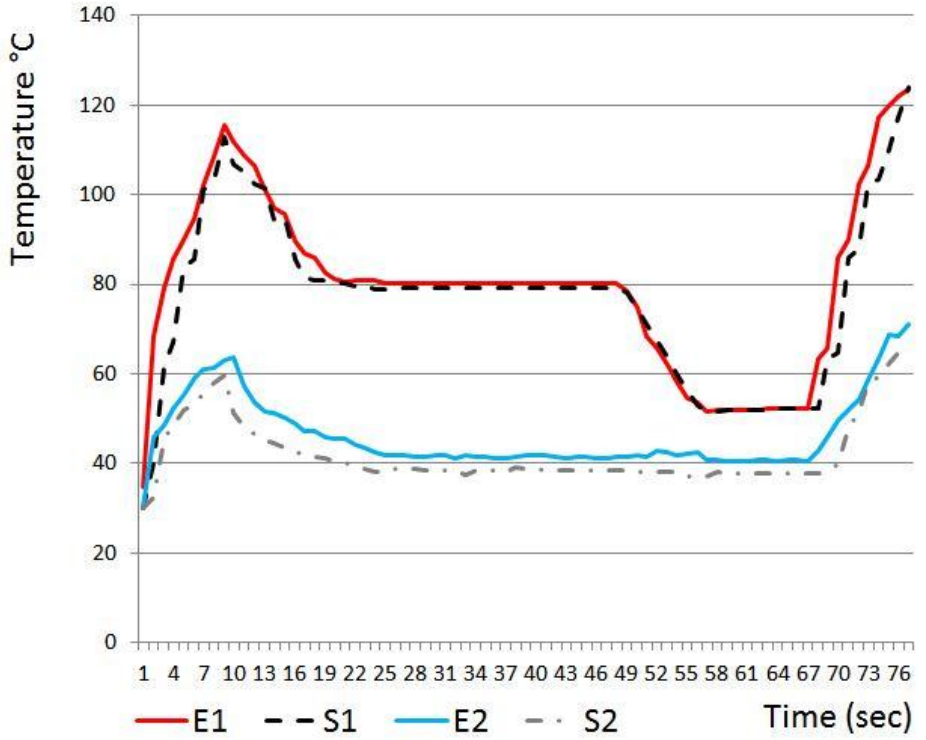

Figure 16 Time-temperature curves of the egg shell measured and calculated for treatment 5. (E1 – measured temperature of shell egg over the air cell, E2 – measured temperature of shell egg on the equatorial part, S1 – calculated temperature of shell egg over the air cell, S2 - calculated temperature of shell egg on the equatorial part)

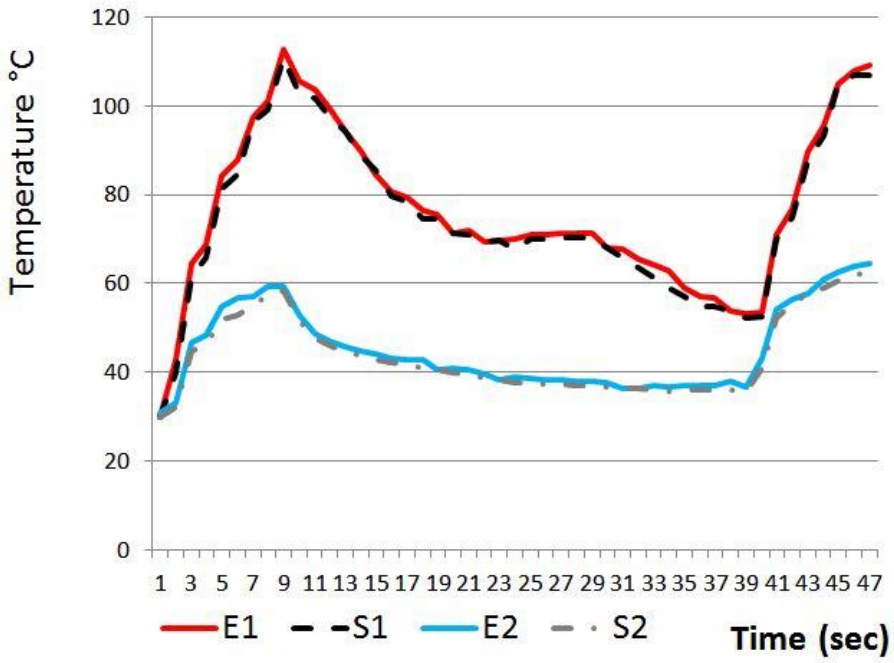

Figure 17 Time-temperature curves of the egg shell measured and calculated for treatment 6. (E1 – measured temperature of shell egg over the air cell, E2 – measured temperature of shell egg on the equatorial part, S1 – calculated temperature of shell egg over the air cell, S2 - calculated temperature of shell egg on the equatorial part)

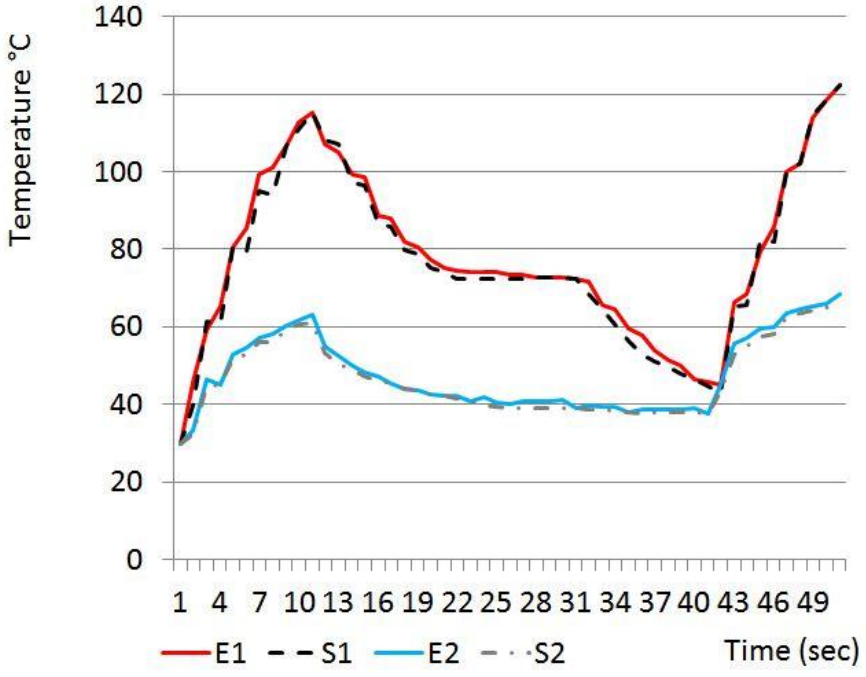

Figure 18 Time-temperature curves of the egg shell measured and calculated for treatment 7. (E1 – measured temperature of shell egg over the air cell, E2 – measured temperature of shell egg on the equatorial part, S1 – calculated temperature of shell egg over the air cell, S2 - calculated temperature of shell egg on the equatorial part)

I.1.5. References

ASTM (1993) Standard test methods for measuring and compensating for emissivity using infrared imaging radiometers. *Annual Book of ASTM Standards*.

Bell, C., & Kyrikides, A.. (2002) Salmonella. *Blackwell Science Ltd*., London

Berrang, M. E., Cox, N. A., Frank, J. F., & Buhr, R. J. (1999). Bacterial penetration of the eggshell and shell membranes of the chicken hatching egg: A review. *Journal of Applied Poultry Research, 8,* 499–504.

Bin, X., & Da-Wen, S. (2002). Applications of computational fluid dynamics (CFD) in the food industry: a review. *Computers and Electronics in Agriculture, 34*, 5-24.

Board, R. G. (1966). Review: The course of microbial infection of the hen's egg. *The Journal of Applied Bacteriology, 29*, 319–341.

Cevoli, C., Fabbri,A., Pasquali, F., Berardinelli,A., Guarnieri, A. (2010). Hot air treatment, in natural convection conditions, for egg surface decontamination. *Journal of Agricultural Engineering 4*, 23-27

Coburn, B., Grassi, G. A., & Finlay, B. B. (2007). Salmonella, the host and disease: A brief review. *Immunology and Cell Biology, 85*, 112–118.

Davies, R.H. and Breslin, M. (2002). Investigations into possible alternative decontaminationmethods for Salmonella enteritidis on the surface of table eggs. *Journal of Veterinary Medicine B. 50,* 38–41.

European Food Safety Authority (2005). Opinion of the Scientific Panel on Animal Health and Welfare on a request from the Commission related to the welfare aspects of various systems of keeping laying hens. The welfare aspects of various systems of keeping laying hens. *EFSA Journal 197*, 1-23

European Food Safety Authority. (2007). Report of the Task Force on Zoonoses Data Collection on the Analysis of the baseline study on the prevalence of Salmonella in holdings of laying hen flocks of Gallus gallus. *The EFSA Journal, 97*

European Food Safety Authority. (2012). Scientific Opinion on a review on the European Union Summary Reports on trends and sources zoonoses, zoonotic agents and food-borne outbreaks in 2009 and 2010 – specifically for the data on Salmonella, Campylobacter, verotoxigenic Escherichia coli, Listeria monocytogenes and foodborne outbreaks

Fabbri, A., Cevoli, C., Giunchi, A. (2010). Validation of a simplified Numerical Model for Hot Air Treatment of Egg Shell Surface, *Food Process Engineering, 35*, 695-700.

Flir (2010) The ultimate infrared handbook for R&D professionals.

Food and Agriculture Organization of the United Nations - FAO, (2010). Poultry, meat & eggs. Agribusiness handbook

Foster, A.M., Ketteringham, L.P., Swain, M.J., Kondjoyan, A., Havet, M., Rouaud, O., Evans, J.A., (2006). Design and development of apparatus to

provide repeatable surface temperature-time treatments on inoculated food samples. *Journal of Food Engineering, Vol. 76*, p. 7 - 18.

Hou, H., Singh, R.K., Muriana, P.M. and Stadelman,W.J. (1996). Pasteurisation of intact shell eggs. *Food Microbiology 13,* 93–101.

James, C., Lechevalier,V. and Ketteringham, L. (2002). Surface pasteurisation of shell eggs. *Journal of Food Engineering 53,* 193–197.

Lamprecht, I., Schmolz, E., Hilsberg, S., Schlegel, S., (2002). A tropical water lily with strong thermogenic behaviour-thermometric and thermographic investigations on Victoria cruziana. *Thermochimica Acta 382,* 199–210.

Mead, P.S., Slutsker, L., Dietz, V., McCaig, L.F., Bresee, J.S., Shapiro, C., Griffin, P.M., &. Tauxe, R.V. (1999). *Food-related illness and death in the United States. Emerging Infectious Diseases 5,* 607-625.

Manfreda, G., Cevoli, C., Lucchi, A., Pasquali, F., Fabbri, A., Franchini, A. (2010). Hot air treatment for surface decontamination of table eggs. *Food Control 21,* 431–435

Miyamoto, T., Horie, T., Baba, E., Sasai, K., Fukata, T., & Arakawa, A. (1998). Salmonella penetration through eggshell associated with freshness of laid eggs and refrigeration. *Journal of Food Protection, 61,* 350–353.

Mori, M, Novak, L., Sekavecnik, M., Kustrin, I (2008). Application of IR thermography as a measuring method to study heat transfer on rotating surface. *Forsch Ingenieurwes 72,* 1–10

Musgrove, M.T., Jones, D.R., Northcutt, J.K., Harrison, M.A.,Cox, N.A. JR, Ingram, K.D. and Hinton, A. JR. (2005). Recovery of salmonella from commercial shell eggs by shell rinse and shell crush methodologies. *Poultry Science 84*, 1955–1958.

Narushin V.G., (1997). The avian egg: geometrical description and calculation of parameters, *Journal of Agricultural Engineering Research, 68*, 201-205.

Olsson, E.E.M., Ahrn, L.M. and Tragardh, A.C. (2004). Heat transfer from a slot air jet impinging on a circular cylinder. *Journal of Food Engineering 63*, 393–401.

Pasquali, F., Fabbri, A., Cevoli, C., Manfreda, G. and Franchini, A. (2009). Hot air treatment for surface decontamination of table eggs. *Food Control 21*, 431–435.

Popoff, M.Y., J. Bockemül, &. Brenner F.W. (1998) Supplement 1997 (no. 41) to the Kauffmann-White scheme. *Research in Microbiology. 149*, 601-604.

Raithby G.D., Terry K.G., (2000) Convection Heat Transfer CRC Handbook of Thermal Engineering. Ed. Frank Kreith, 2000, Boca Raton: CRC Press LLC.

Regulation (EC), (2004), No 853 Official Journal of the European Union.

Romane, A., Harrak, R. and Bahri, F. (2012). Use Thyme Essential Oils for the Prevention of Salmonellosis, Salmonella - A Dangerous Foodborne Pathogen, Dr. Dr. Barakat S M Mahmoud, *InTech*.

Stadelman, W. J., Singh, R. K., Muriana, P. M., & Hou, H. (1996). Pasteurisation of eggs in the shell. *Poultry Science, 75*, 1122–1125.

Van der Plancken, I.,Van Loey, A. and Hendrickx, M.E. (2005). Effect of heat-treatment on the physico-chemical properties of egg white proteins: a kinetic study. *Journal of Food Engineering. 75*, 316–326.

World Health Organization (2005). Drug-Resistant Salmonella. WHO website.

World Health Organization/Food and Agriculture Organization of the United Nations (WHO/FAO), (2002). Risk assessments of Salmonella in eggs and broiler chickens. Microbiological risk assessment series. FAO website

II.2 Application of infrared thermography for controlling freezing process of raw potato

This paper was written by Cuibus, L.[1], Fito, P.J.[2], Fabbri, A[1], Castro-Giráldez, M.[2*] and was send to Journal of Food Engineering.

Application of infrared thermography for controlling freezing process of raw potato

Cuibus, L.[1], Fito, P.J.[2], Fabbri, A[1], Castro-Giráldez, M.[2*]

1 Dep. of Agricultural and Food Science, University of Bologna, Piazza Goidanich 60, 47521 Cesena (FC)

2 Instituto Universitario de Ingeniería de Alimentos para el Desarrollo, Universidad Politécnica de Valencia, Camino de Vera s/n, 46022 Valencia, Spain

**Author for correspondence: marcasgi@doctor.upv.es*

Freezing technique is a very useful method for food preservation. The distribution of temperatures of raw potato was measured during the freezing operation by using an infrared thermographic camera Thermal Imager Optris PI160. Moreover, moisture was measured before and after the freezing process. Differential Scanning Calorimetry of potato was also measured to analyze the freezing process. The aim of this work was to analyze the potato freezing process by using infrared thermography; the results showed that infrared thermography can be considered an important nondestructive tool for controlling the freezing process of potato.

Keywords: infrared thermography, potato, freezing.

II.2.1 Introduction

Freezing is one of the most important methods for food preservation which produces good quality and long shelf-life food products (Delgado & Sun, 2001). The phase transitions of the freezing process involve the conversion of water to ice through the crystallization process (Fennema et al., 1973; Alizadeh et al., 2009; Kiani & Sun, 2011). The extracellular large ice crystals produce a significant damage to the food tissue (Sun & Zheng, 2003). The formation of fine crystals, distributed inside and outside the cells, leads to a high quality product that can be better preserved because the tissue has been less damaged (Sun & Zheng, 2006; Kiani & Sun, 2011). Usually, the slow freezing produces large ice crystals, while rapid freezing produces small intracellular ice (Li & Sun, 2002 a, b). To improve the control of freezing process, it is necessary to understand the crystallization process and the thermodynamic properties of water. In many fields, the infrared thermography (TI) becomes a non-destructive and non-contact technique commonly used for measuring the temperature of the products. TI is a two-dimensional, non-contact diagnostic technique for measuring surface temperature of materials which can be usefully used in non-destructive quality evaluation (Giorleo & Meola, 2002, Gowen & all, 2010). The radiometric surface temperatures obtained from thermal camera measurements are related with both the physical surface temperature and the effective emissivity of the surface within the band pass of the radiometric measurements (Humes et al., 1994; Lopez et al., 2012). The emissivity describes the ratio of radiation emitted by an object at a certain temperature, to the value emitted by a perfect emitter (Husehke, 1959; Lopez et al., 2012).

The aim of the present study is to monitor the dynamics of variation of emissivity of potato during the freezing process. This paper may offer a good opportunity of food processors to realize the control of freezing potato using an infrared thermocamera.

II.2.2 Material and methods

Experimental procedure

It is fundamental to calibrate properly the infrared sensor in order to obtain reliable data of temperature. For this reason, previous experiments were carried out with reference materials (ε=0.95) in order to obtain a real value of emissivity. Experimental setup consisted on potato sample, distilled water and an aluminium foil. Fresh potato samples (Solanum tuberosum L. cv. Melody) were peeled and cut with a cylindrical core borer in order to obtain cylinders with 20 mm diameter and 10 mm height. Distilled water was placed in a box with a bottom half painted with black color (emissivity close to 1) and the other half was covered with aluminium, although no differences were found between both measurements. The freezing process was carried out from 20ºC until -20ºC with freezing air velocity of 0.45 m/s. The experimental was carried out by triplicate but only one of them is shown as an example.

A thermographic camera Thermal Imager Optris PI160 with a spectral infrared range of wavelength from 7.5 a 13 μm was used for the experiments. Moreover, different thermocouples (Thermometer model HIBOK 14) were used to register the temperature of potato surface, water, aluminium foil and ambient. *Figure 19* shows an scheme of the experimental setup.

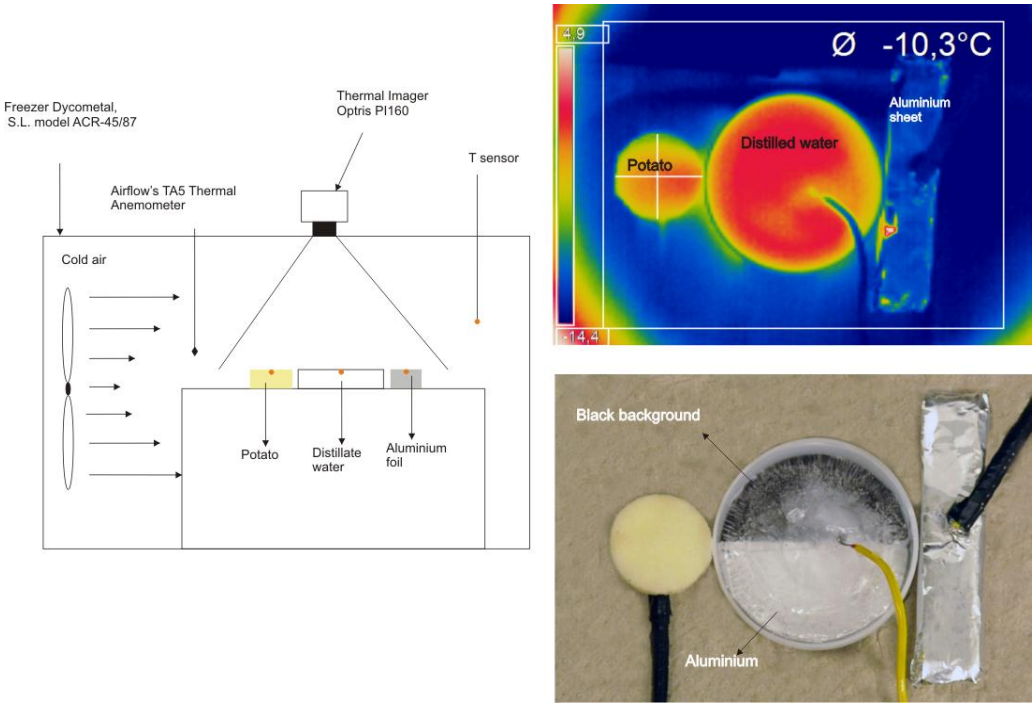

Figure 19 Experimental setup.

Moisture was measured before and after the freezing process according to the AOAC (1984) method 22.013.

Study of phase transitions: Differential Scanning Calorimetry (DSC)

Phase transitions were measured using a DSC 220 CU-SSC5200 (Seiko Instruments) connected to a cooling controller. Samples of around 15-20 mg were enclosed in hermetically sealed aluminum pans (Seiko Instruments, P/N SSC000C008) and then loaded into the equipment at room temperature. An empty hermetically sealed pan was used as the reference sample. The calibration of the cell was made following the DSC manufacturers' recommendation. Samples were cooled from 20ºC to -60ºC and heated from -60ºC to 20ºC. Heating scans were performed at 10ºC/min. The DSC measurements were made by triplicate.

II.2.3 Results and discussion

Figure 20 shows the freezing curve of pure water, potato and aluminium foil obtained by the thermocouples. In the freezing curve of water, a slight supercooling can be observed reaching -2ºC; at this point, the crystal nucleation starts and an abrupt rise from the supercooled temperature to near 0ºC occurs caused by the release of the latent heat of crystallization. The freezing process continue forming ice crystals until around -4ºC; at this point, all the water has been transformed into ice and the temperature of the ice mass starts to decrease until -18ºC (equilibrium temperature). The figure also shows the curve of potato freezing; this curve shows a freezing temperature of -2ºC due to the large amount of solutes found in this system. When part of the potato water starts to be crystallized, the potato liquid phase is being concentrated causing a decrease of the water freezing point. The aluminium cooling curve shows a rapid decrease of the temperature reaching in less than ten minutes the equilibrium temperature. This reference material does not suffer any transition at these temperatures.

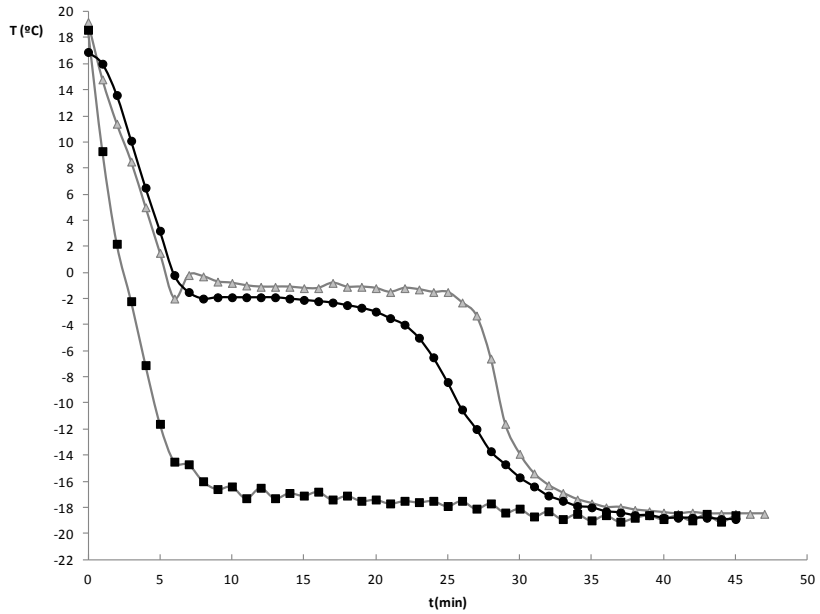

Figure 20 Freezing curves for potato (●), water (▲), and aluminium (■)

All the objects with temperature above the absolute zero emit thermal radiation following the Stefan-Boltzman law. In the present study, the infrared camera registers the thermal energy emitted by the different bodies inside the freezer, graphing a map of temperatures. In this case, the emissivity value used for register the temperatures by the IR camera was 0.98 which is a common emissivity for cellular tissues. Due to the fact that the emissivity of the bodies is changing with the freezing treatment, the map of temperatures obtained by the camera is not real, and thus, the temperatures were converted into thermal energies, which can be considered as the response of the camera pyrosensor to the radiant energy in the infrared spectrum; the radiant energy that can be absorbed by the pyrosensor corresponds to the energy emitted by the superior orbital of the bodies that are inside the freezer. The overall energy received by the camera can be defined by equation II.3:

$$E_T = \varepsilon_S \sigma T_S^{\,4} = F \cdot \varepsilon_{obj} \sigma T_{obj}^4 + (1-\varepsilon_{sur}) \sigma T_{sur}^4 + (1-\tau_{air}) F \cdot \varepsilon_{obj} \sigma T_{obj}^4 + E_{Ch} \quad \text{(II.3)}$$

Where E_T is the overall energy received by the pyrolysis sensor, F is a geometric factor, being 1 because the potato surface is located in parallel with the camera, ε is the emissivity (from the object, surroundings or fixed in the camera), σ the constant of Stefan-Bolzman ($5{,}67 \cdot 10^{-8}$ W/m^{2}K), T the temperature (from the object, surroundings or obtained in the IR camera) and E_{Ch} is the energy emitted in a first order transition or chemical reaction. First term represents the energy emitted by the potato; the second emitted by the surroundings and the third represents the energy absorbed by the air.

As the freezer chamber is completely sealed and black, it can be considered that there is no energy reflected from the environment, so all the energy that arrives to the IR camera comes from the potato, water and aluminium foil. This means, that

only the energy emitted by the object is considered, being neglected the background radiation and the atmospheric contribution. This fact was corroborated by a previous experiment in which a reference grey body was located inside the freezer, and the emissivity registered was 0.95 in all the temperature range of study.

Figure 21 shows the changes in the energy received by the camera with regard to the temperature measured by the thermocouples. In the figure it is possible to appreciate that the energy received by the camera has the same tendency for potato and for pure water. It is also possible to appreciate that the energy decreases in three different steps, being possible to detect the freezing process. This can be better appreciated in *figure 22*.

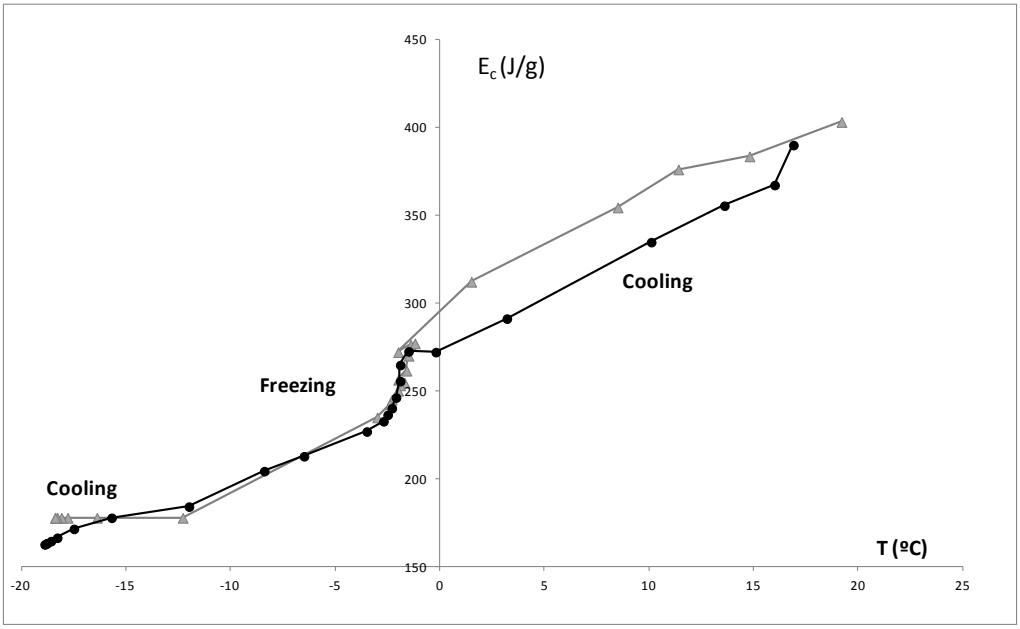

Figure 21 Energy received by the camera with regard to the temperature of (●) potato and (▲) water.

In *figure 22*, the energy received by the camera shows three different slopes which define the different steps in the freezing process of potato: the cooling until the

freezing temperature, the freezing and the crioscopic decrease, and the cooling of the frozen product. *Figure 23* shows the same steps for water freezing process.

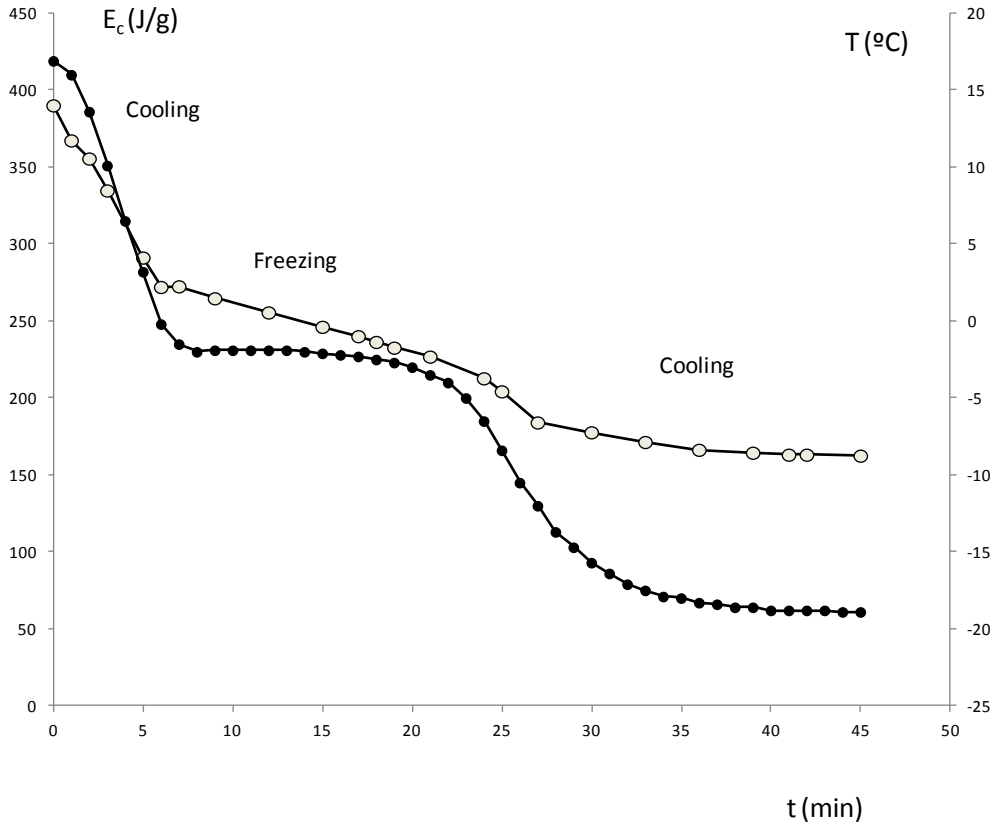

Figure 22 Freezing curve for potato (●), compared with the energy emitted by the potato and registered by the camera thorough the treatment (○).

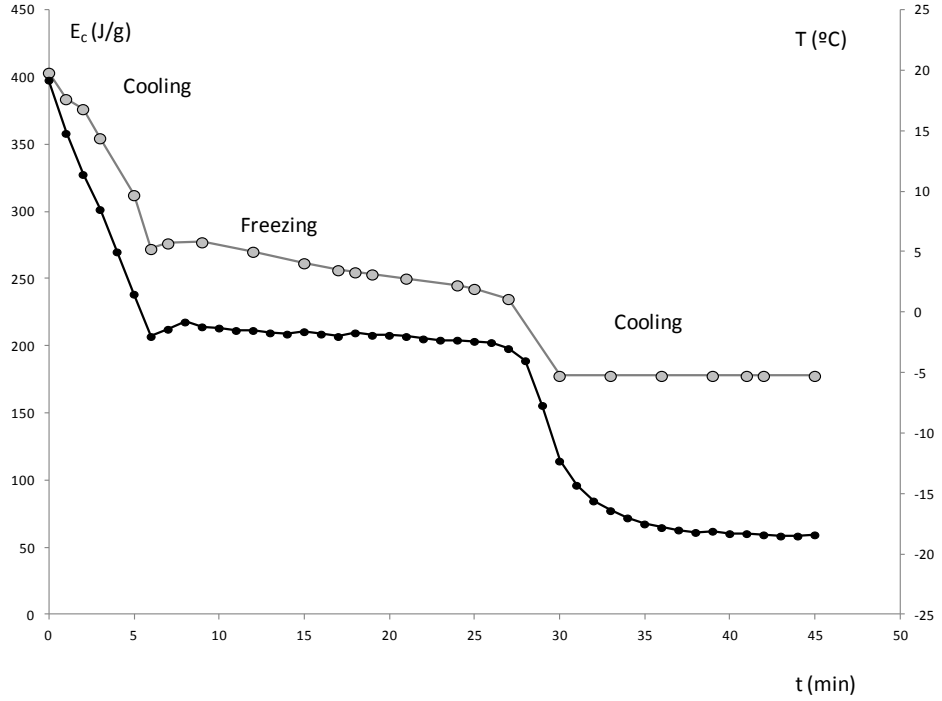

Figure 23 Freezing curves for water (●), compared with the energy emitted by the potato and registered by the camera thorough the treatment (●).

The thermal energy of the potato registered by the camera could be related with the internal energy, which is the energy that depends on the state of the molecules orbitals. From the data obtained by differential Scanning Calorimetry, the specific heat was obtained in the sections without transitions. *Figure 24* shows an example of potato thermogram.

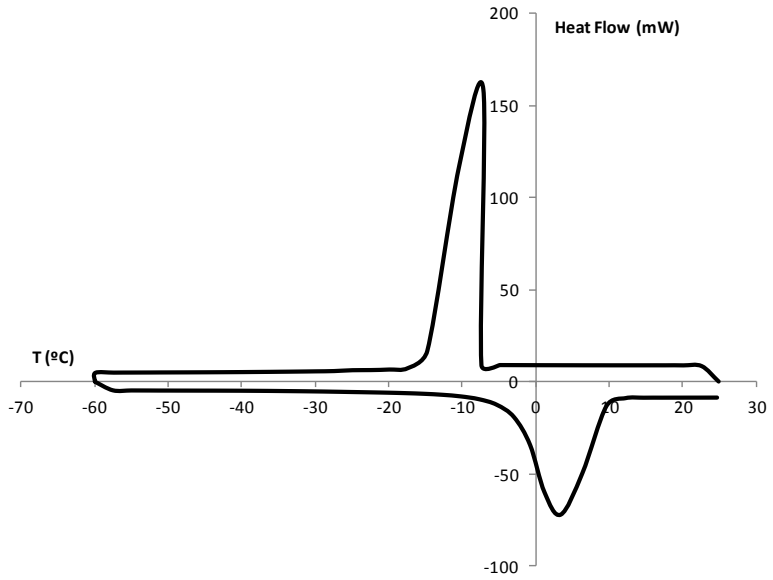

Figure 24 Differential scanning calorimetry thermogram of potato.

Internal energy of potato (U) was calculated as follows:

$$U = mC_P\left(T - T_{ref}\right) \qquad \text{(II. 4)}$$

where, Cp is the specific heat obtained by thermography for the potato, and obtained from bibliographic sources for the pure water (Heldman and Lund, 2007). T is the temperature of potato and water measured at each time with the thermocouples, and T_{ref} is the temperature of reference which was considered as 0ºC.

The three different steps mentioned before can be observed as well in *figure 25*. In the figure it is possible to appreciate that, in the freezing process, the internal energy does not varies significantly but the energy emitted by the potato shows a marked decrease.

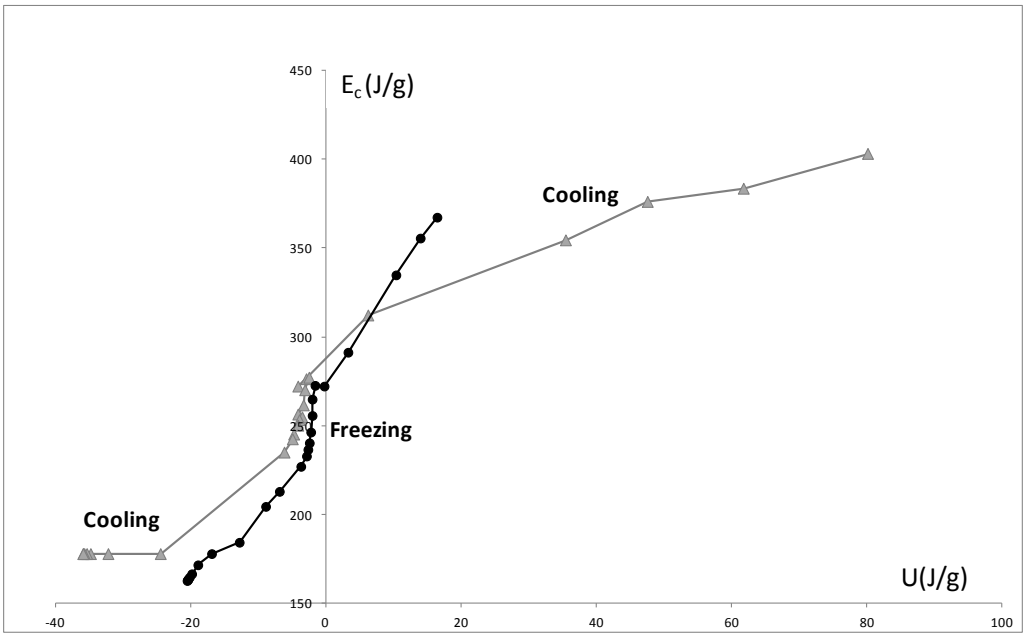

Figure 25 Energy received by the camera with regard to the internal energy of potato (●) and water (▲).

Considering only the potato freezing, it is possible to estimate the crystallization enthalpy from *figure 26*, plotting a straight line on the stages of cooling (without transitions).

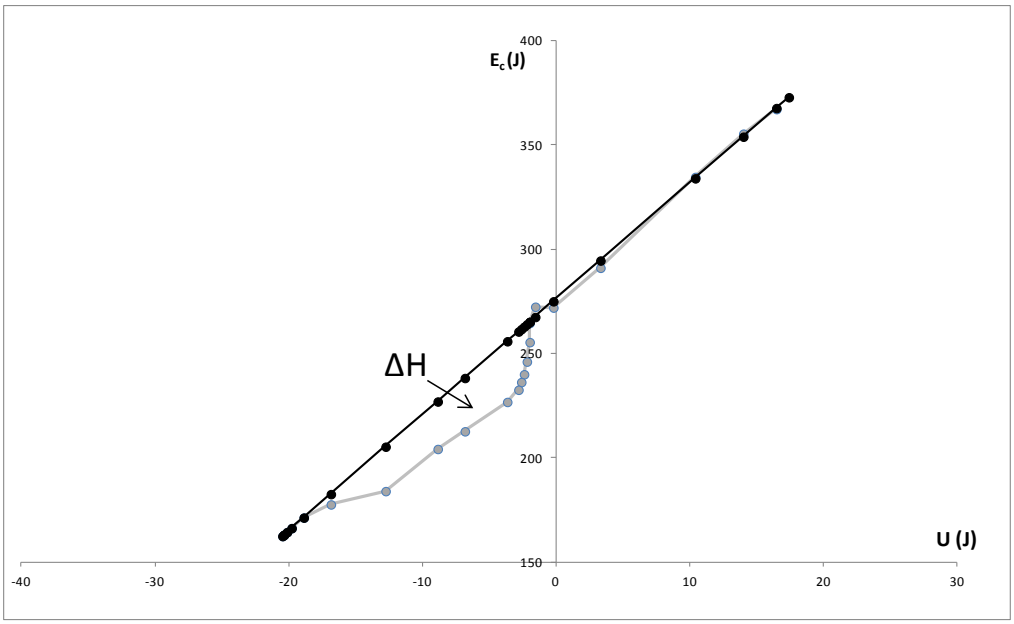

Figure 26 Energy received by the camera with regard to the internal energy of potato (●) and water (▲).

By other hand, with the melting enthalpy of potato (see table 4) obtained from the calorimetric analysis and the melting enthalpy of pure water obtained from the bibliography, it is possible to obtain the unfreezeable water (x_w^{nf}) (Sablani et al., 2009).

Table 4 Results from the DSC experiments, moisture and non freezeable water estimated

$\Delta H_{melting}$	$\Delta H_{freezing}$	ΔH_{water}	Tm'	x_w^0	x_w^{nf}
223±15	249±19	334	-19±2	0.847±0.015	0.204±0.016

Comparing the enthalpy obtained from *figure 26* with the crystallization enthalpy of pure water, it is possible to estimate freezing enthalpy area and also the quantity of ice formation following the energies involved in the emission of molecules (*Figure 27*). By subtracting the amount of ice formed to the initial moisture of the samples, it is possible to obtain the amount of water that remains in liquid phase (*Figure 27*). In the figure, it is possible to appreciate that the amount of water that remains in liquid phase reaches a value near 0.2 that coincides with the value of unfreezeable water obtained by DSC. It is also possible to observe that the temperature of the potato remains during the whole treatment below the Tm', and, thus, ice is being formed during all the treatment.

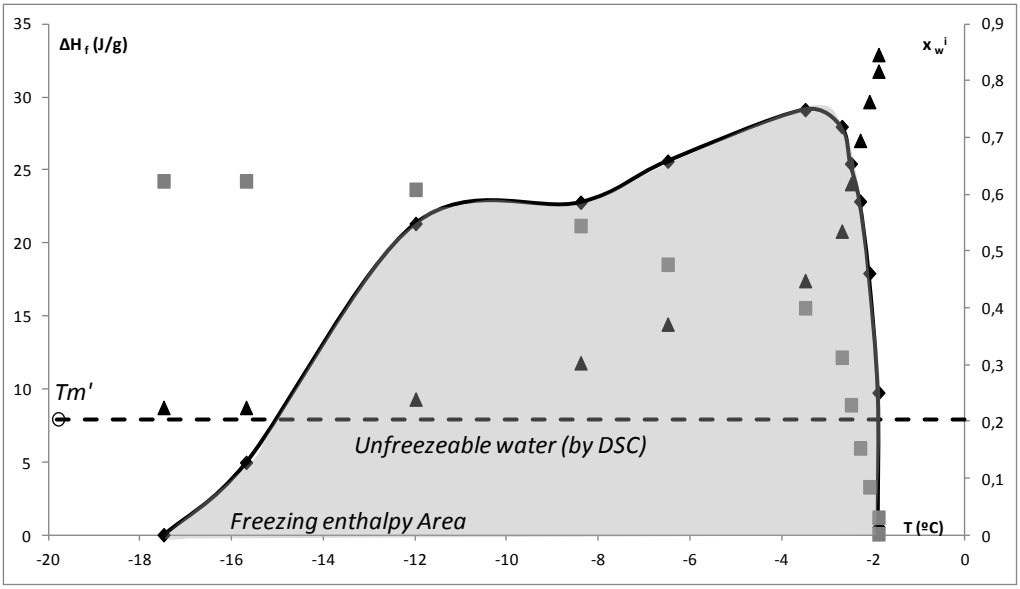

Figure 27 Freezing enthalpy area with regard to the temperature (principal axis); water mass fraction (x_w^i) with regard to the temperature (secondary axis), where super index "i" represents the liquid state (▲) or ice state (■).

The real emissivity of potato was calculated during the freezing process. The procedure to calculate the emissivity is explained next:

$$\varepsilon_{suposed} \rightarrow E_C = \sigma T_{calculated}^{\ 4} \varepsilon_{suposed}$$

$$f(error) = \sum (T_{calculated} - T_{measured})^2 \rightarrow \varepsilon_P$$

With this procedure the real emissivity of potato was obtained for the freezing process. *Figure 28* shows the emissivity evolution during the freezing process.

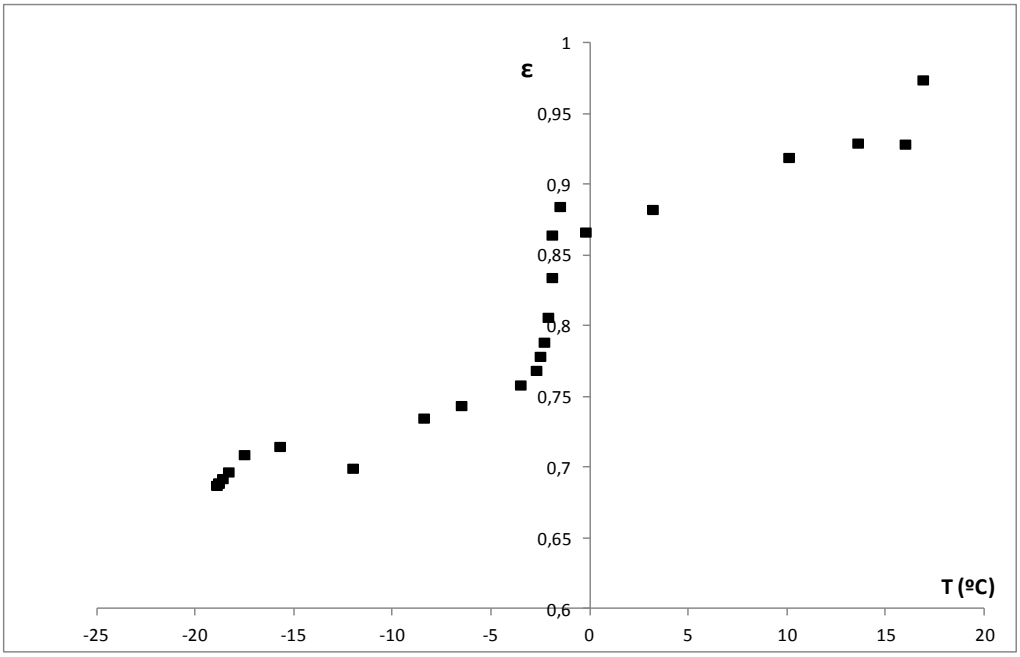

Figure 28 Emissivity with regard to temperature for potato (■).

Conclusions

The results showed that infrared thermography can be considered an important nondestructive tool for controlling the freezing process of potato. This technique can be used to describe completely the freezing potato process, being possible to calculate the quantity of ice formed and the emissivity of the potato during this process.

II.2.4 References

Aguilera, L. M., & Stanley, D. W. (1990). Microstructural principles of food processing and engineering. Essex, UK: *Elsevier Science Publishers Ltd.*

Alizadeh, E., Chapleau, N., de Lamballerie, M., & Le-Bail, A. (2007). Effect of different freezing processes on the microstructure of Atlantic salmon (Salmo salar) fillets. *Innovative Food Science & Emerging Technologies, 8,* 493-499.

Alvarez, M., Fernandez, C., & Canet, W. (2010). Oscillatory rheological properties of fresh and frozen/thawed mashed potatoes as modified by different cryoprotectants. *Food and Bioprocess Technology, 3,* 55 - 70.

AOAC (1984). Official methods of analysis (14^{th} ed.). Washington, DC: Association of Official Analytical Chemists.

Buettner, K.J.K., Kern, C.D., (1965). The determination of infrared emissivities of terrestrial surfaces. *Journal of Geophysical Research 70,* 1329–1337.

Da-Wen Sun *, Bing, Li, (2002). Microstructural change of potato tissues frozen by ultrasound-assisted immersion freezing, *Journal of Food Engineering*

Delgado, A. E., & Sun, D.-W. (2001). Heat and mass transfer models for predicting freezing process—a review. *Journal of Food Engineering, 47,* 157–174.

Fennema, O. R., Powrie, W. D., & Marth, E. H. (1973). Low temperature preservation of foods and living matter. *New York: Marcel Dekker.*

Fellows, P. (2000). Food Processing Technology—Principles and Practice (2nd ed., pp. 418–440). Chichester, UK: *Ellis HorwoodLtd*.

Fuller M. P. and Wisniewski M., (1998). The use of infrared thermal imaging in the study of ice nucleation and freezing of plants *Journal of Thermal Biology* Vol. 23, No. 2, pp. 81-89.

Gowen, A. A., Tiwari, B.K., Cullen, P.J., O'Donnell, C.P., McDonnell, K. (2010). Applications of thermal imaging in food quality and safety assessment. *Trends in Food Science & Technology* 21 (2010) 190e200

Giorleo, G., & Meola, C. (2002). Comparison between pulsed and modulated thermography in glasseepoxy laminates. *NDT & E International*, 35(5), 287e292.

Hudson, M.A. and Idle, D.,B. (1962). The formation of ice in plant tissues. *Planta 57*, 718-730

Jalté M., Lanoisellé J.L., Lebovka, N. I., & Vorobiev, E. (2007). Plasmolysis of sugarbeet: pulsed electric fields and thermal treatment. *LWT - Food Science and Technology* 42 (2009) 576–580

Karlsson, M.E. & Eliasson A.-C. (2003). Gelatinization and retrogradation of potato (Solanum tuberosum) starch in situ as assessedby differential scanning calorimetry (DSC) *Lebensm.-Wiss. u.-Technol*. 36, 735–741

Kiani, H. and Sun. D-W, (2011) Water crystallization and its importance to freezing of foods: A review. *Trends in Food Sscience & Technology 22*, 407-426

Kita, A. (2002). The influence of potato chemical composition on crisp texture, *Food Chemistry* 76,173-179

Le Grice, P., Fuller, M. P. & Campbell, A. (1993). An investigation of the potential use of thermal imaging technology in the study of frost damage to sensitive crops. *Proceedings of 6th International Conference on Biological Ice Nucleation. University of Wyoming*, Laramie, USA, p. 4.

Li, B., & Sun, D.-W. (2002 a). Novel methods for rapid freezing and thawing of foods—a review. *Journal of Food Engineering*, 54, 175–182.

Li, B.,& Sun, D.-W. (2002 b). Effect of power ultrasound on freezing rate during immersion freezing. *Journal of Food Engineering*, 55, 85–90.

Lopez, A., Molina-Aiz, F.D., Valera, D.L. & Pena, A., (2012). Determination the emissivity of the leaves of nine horticultural crops by means of infrared thermography. *Scientia Horticulturae 137*, 49 - 58

Minkina, W. (2004). Thermovision Measurements – Instruments and Methods, *Publishing Office of Częstochowa University of Technology, Częstochowa,* (in Polish)

Pinkley, L.W., Sethna, P.P., Williams, D., (1977). Optical constants of water in the infrared: influence of the temperature. Journal for Optical Society of America 67 (4), 494–499.

Robinson, P.J., Davies, I.A., (1972). Laboratory determinations of water surface emissivity. *Journal of Applied Meteorology 11*, 1391–1393.

Sablani, S.S., Bruno, L., Kasapis, S. & Symaladevi, R.M. (2009). Thermal transitions of rice: development of a state diagram. *Journal of Food Engineering*, 90, 110-118.

Singh, J., Kaur, L. (2009). Advances in potato chemistry and technology, *Academic Press, Elsevier Inc*.

Sun, D.-W., & Li, B. (2003). Microstructural change of potato tissues frozen by ultrasound-assisted immersion freezing. *Journal of Food Engineering, 57*, 337 - 345.

Sun, D.-W., & Zheng, L. (2006). Innovations in freezing process. In D. W. Sun (Ed.), Handbook of frozen food processing and packaging. *Boca Raton, Fla./London: CRC/Taylor & Francis*.

Świędrych, A., Prescha, A., Matysiak-Kata, I., Biernat, J., Szopa, J. (2002). Repression of the 14-3-3 gene affects the amino acid and mineral composition of potato tubers, *Journal of agricultural and Food Chemistry*, 50, 2137-2141

Szymońska, J., & Wodnickab, K. (2005). Effect of multiple freezing and thawing on the surface and functional properties of granular potato starch, *Food Hydrocolloids* ,753–760

Wisniewski, M., Lindow, S. E. & Ashworth, E. N. (1997). Observations of ice nucleation and propagation in plants using infrared video thermography. *Pl. Phys*. 113, 327-346.

Zhang, Y.W., Zhang, C.G., Klemas, W., (1986). Quantitative measurements of ambient radiation, emissivity, and truth temperature of a greybody: methods and experimental results. Applied Optics 28 (20), 4482–4486.

II.3 Analysis of water motion throughout the potato (var. Melody) freezing by infrared thermography, microstructural and dielectric techniques.

This paper was written by Cuibus, L.[1], Castro-Giráldez, M.[2], Fabbri, A[1], Fito, P.J.[2*] and was send to Journal of Food Engineering.

Analysis of water motion throughout the potato (var. Melody) freezing by infrared thermography, microstructural and dielectric techniques.

Cuibus, L.[1], Castro-Giráldez, M.[2], Fabbri, A[1], Fito, P.J.[2*]

1 Dep. of Agricultural and Food Science, University of Bologna, Piazza Goidanich 60, 47521 Cesena (FC)

2 Instituto Universitario de Ingeniería de Alimentos para el Desarrollo, Universidad Politécnica de Valencia, Camino de Vera s/n, 46022 Valencia, Spain

**Author for correspondence: pedfisu@tal.upv.es*

The Freezing process so used in the industries to preserve sometimes produces damages in the product. The distribution of temperatures of raw potato was measured during the freezing operation by using an infrared thermographic camera Thermal Imager Optris PI160. Moreover, volume, moisture and water activity were measured before and after the freezing process. Cryo-SEM was also used to analyze the microstructure of potato before and after freezing. The dielectric spectra of potato samples were measured before freezing and after defreeze, using an Agilent 85070E Open-ended Coaxial Probe connected to a network analyzer Agilent E8362B in the frequency range from 500 MHz to 20 GHz. The aim of this work was to control the temperature of potato surface during

the freezing operation to determine the water chemical potential and structural changes of potato during this process, in order to determine the water motion throughout the freezing. The results showed important relations between the heat flux, water chemical potential gradients, structure changes and dielectric properties indicating that infrared thermography and dielectric properties can be considered very important nondestructive tools for controlling the freezing process of potato.

II.3.1 Introduction

The potato (Solanum tuberosum L.) which is grown in over 100 countries throughout the world is one of the staples of the human diet and one of the most important raw materials for the food industry. Potatoes are one of the most important sources of energy and other nutrients including vitamins and minerals (Singh & Kaur, 2009). Potatoes are industrially processed in a wide range of convenience products (Karlsson & Eliasson, 2003). The dry matter of potato tubers is composed of various substances: starch (15%), sugars, nitrogen compounds, lipids, organic acids, phenolic compounds, mineral substances and non-starch polysaccharides (protopectin, soluble pectin, hemicelluloses, cellulose) (Kita, 2002).

Freezing is one of the most used methods for long preservation of food products, because it results in minimal deterioration of the original flavour, colour, texture or nutritional values (Jalté& all, 2007) when it is compared with other preservation methods. The quality of frozen foods depends on the size of ice crystals (Li & Sun, 2002 a, b). Rapid freezing produces small intracellular ice crystals, while slow freezing forms large ice crystals. Large ice crystals would cause damages to food quality including appearance, sensory properties, textural attributes and nutritional value (Li & Sun, 2002). Plant tissues (fruits and vegetables), which present a semi-rigid cellular structure, exhibit less resistance to the expansion of ice crystals in volume, thus they are prone to being subjected to the irreversible freezing damage (Li & Sun, 2002). The freezing damages are also caused by solute concentration in the unfrozen liquid and the osmotic transfer of water from cell interior determines the dehydration damage. These damages in

plant tissues would result in loss of function in cell membrane, disruption of metabolic systems, protein denaturation, permanent transfer of intracellular water to the extracellular environment, enzyme inactivation, and extensive cell rupture (Li & Sun, 2002).

Until recently, the only method for the detection of ice formation in plant tissues has been the electronic recording of plant temperature using thermocouples and examining the exothermic process, but this detection methods are both difficult and sometimes unreliable (Le Grice et al., 1993; Wisniewski et al., 1997). Moreover, the thermocouples are inserted into the tissue damaging the cells and leading to solute leakage which itself may become a site for ice nucleation thus creating an artifact (Le Grice et al., 1993; Wisniewski et al., 1997). Recent advances and potential applications of Infrared thermography (TI) for food safety and quality assessment such as temperature validation bruise and foreign body detection and grain quality evaluation have been reviewed (Gowen& all, 2010). TI is a two-dimensional, non-contact diagnostic technique for measuring surface temperature of materials which can be usefully employed in non-destructive quality evaluation (Giorleo & Meola, 2002, Gowen& all, 2010).

The aim of this paper was to describe and quantify the effect of the motion of water in the freezing process and evaluate it effect in the structure.

II.3.2 Material and methods

Ten Fresh potato samples (Solanum tuberosum L. cv. Melody) were tempered at 4ºC before starting the experiment. Ten fresh potato samples were peeled and cut with a cylindrical core borer in order to obtain cylinders with 45 mm diameter and 70 mm height. Potato samples were removed from the refrigerator, placed in the freezer (Dycometal, S.L. model ACR-45/87) and maintained at -20 ºC. During the freezing process, the surface temperature was recorded with an infrared thermocamera (Thermal Imager optris PI160 with 120 Hz frame rate, detector with 160 x 120 pixels), see *figure 29*. The volume of the samples during freezing process was determined by image analysis of the pictures captured with thermocamera every three minutes. The image analysis was made with Adobe Photoshop®. Moreover, different thermocouples (Thermometer model HIBOK 14) were used to register the temperature of potato surface, the internal temperature of potato and the temperature of the freezer. Volume, mass, surface water activity, sugar content (º Brix), moisture and dielectric properties were measured for every sample before and after freezing process. Mass was determined using a Mettler Toledo (±0.0001) (Mettler-Toledo, Inc., USA) balance.

The surface water activity was measured with hygrometer (DECAGON model Aqualab CX-2, ±0.003). The measurement was carried out at 25ºC. Sugar content was determined with a refractometer (Atago NAR-3T serie No 072505, Japan).

Moisture was determined by drying in vacuum at 70 ºC till constant weight (AOAC, 1990). Cryo-SEM (low temperature scanning electron microscope) was also used to analyzed the microstructure of potato before and after freezing; Cryostage CT-1500C unit (Oxford Instruments, Witney, UK), coupled to a Jeol

JSM-5410 scanning electron microscope (Jeol, Tokyo, Japan) were used for the analysis. The samples of fresh raw potato, respectively unfrozen potato, was immersed in slush N_2 (-210ºC) and then quickly transferred to the Cryostage at 1 kPa, where sample fracture took place. The sublimation (etching) was carried out at -95ºC; the final point was determined by direct observation in the microscope, working at 5 kV. The air velocity was measured using portable Airflow's TA5 Thermal Anemometer.

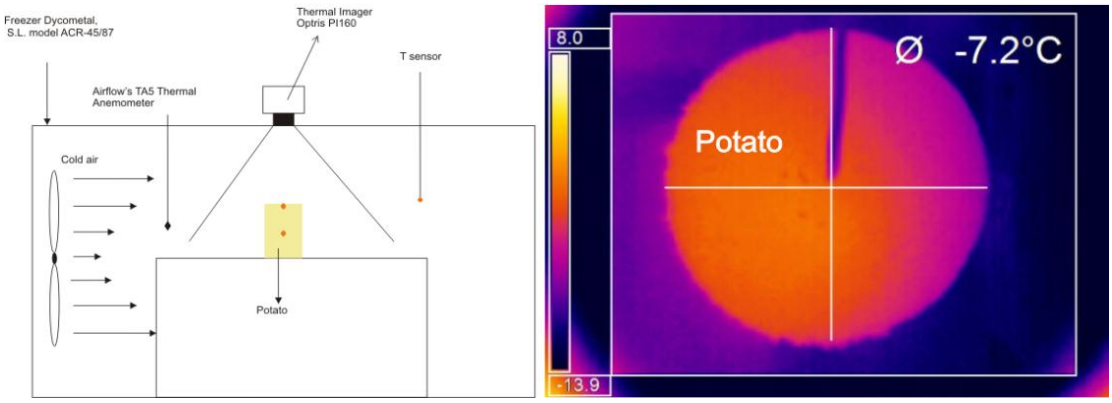

Figure 29 Experimental scheme of freezing process and control system.

II.3.3 Results and discussion

In order to determine the real temperature at the upper surface of the potato during the freezing process, it was estimated the emissivity of each potato in function of the temperature and the freezing process. It has been applied the following equation (see equation II.5)

$$E_T = \varepsilon_S \sigma T_S^{\,4} = F \cdot \varepsilon_{obj} \sigma T_{obj}^4 + (1-\varepsilon_{sur}) \sigma T_{sur}^4 + (1-\tau_{air}) F \cdot \varepsilon_{obj} \sigma T_{obj}^4 + E_{Ch} \quad \text{(II.5)}$$

Where E_T is the overall energy received by the pyrolysis sensor, F is a geometric factor, being 1 because is parallel with the camera, ε is the emissivity (from the object, surroundings or fixed in the camera), σ the constant of Stefan-Bolzman ($5{,}67 \cdot 10^{-8} W/m^2K$), T the temperature (from the object, surroundings or obtained in the IR camera) and E_{Ch} is the energy emitted in a first order transition or chemical reaction. First term represents the energy emitted by the potato; the second emitted by the surroundings and the third represents the energy absorbed by the air.

In order to obtain the real temperature of the object where developed a simple methodology with measures of temperature by thermopar sensor, sited in centre of sample (1 mm of the surface) and was fitted real energy emitted and energy received by the IR camera to obtain temperature profiles of surface sample.

The apparent emissivity was obtained, and it is shown in *figure 30*. In this figure it is possible to observe a low decreasing of emissivity before freezing, fast depression through the ice formation and an increasing of it during the low ice formation and liquid phase concentration process.

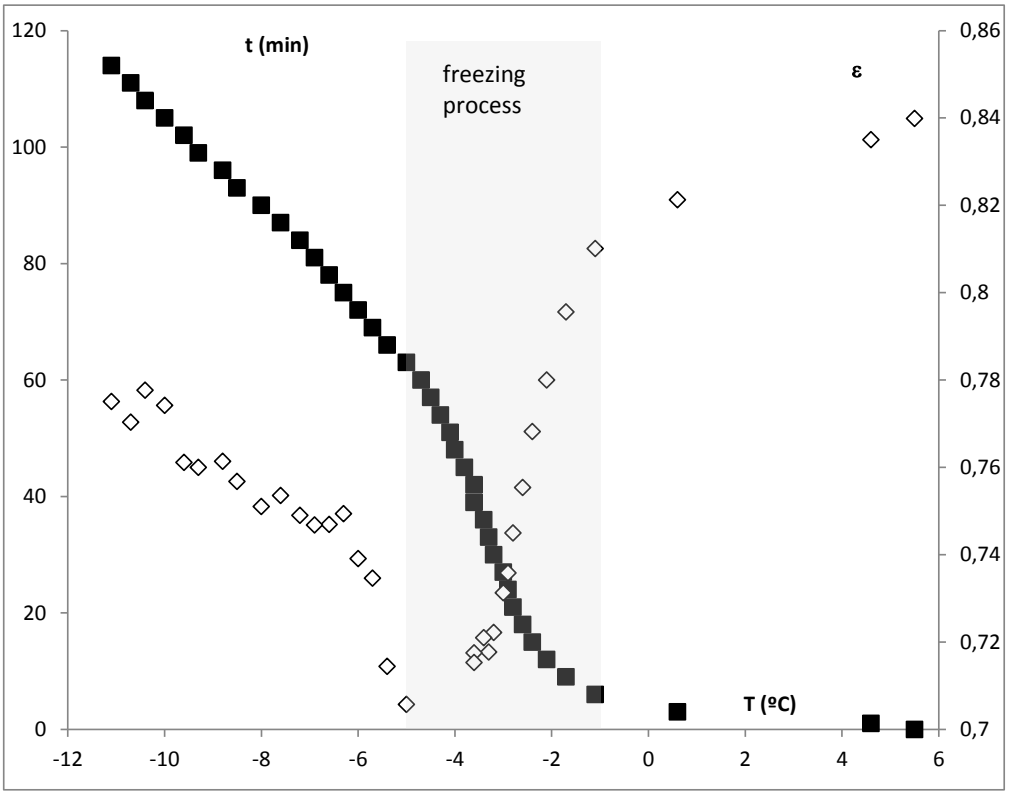

Figure 30 Freezing process curve (■) and relative emissivity values (◊).

With this relation between emissivity and surface temperature is possible to obtain the whole profile of temperatures in the slab surface of potato. *Figure 31* shows an example of temperature profile.

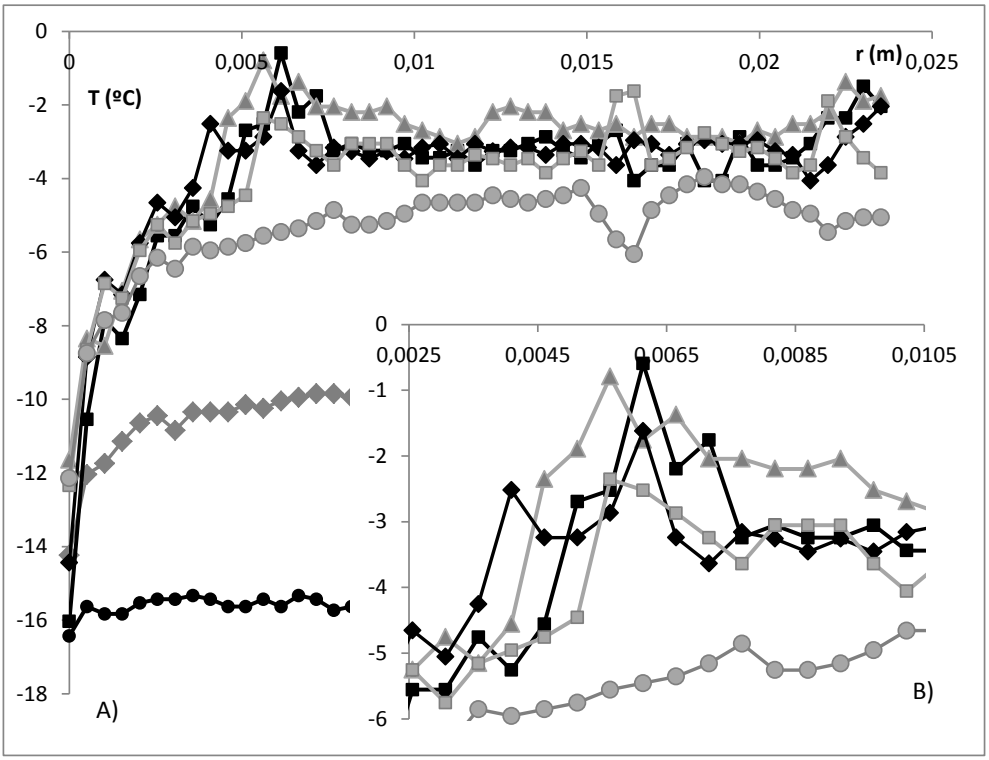

Figure 31 Temperature profile of potato sample through freezing process at 6(▲), 9(■), 12(♦), 42(■), 51(●), 84(♦) and 120 min(●); being distance (r) beginning in the surface.

Figure 31 shows the temperature profiles, where it is possible to observe that, in the first 42 minutes, the shape of the curve appears with peaks at same distances from the cylindrical surface, being the biggest in this sample about 5.5 mm. Those peaks shows flows of heat, but the only possibility to heat from inside to outside is with the water motion from warm to cold zones.

The punctual temperature can also represent in front of freezing process time, in *figure 32*, it is represents for different distances from the surface. Near the surface, the temperature increases the first 20 minutes, then remains approximately constant until the 40 minutes and then decreases. After 5 mm in depth, the temperature is decreasing but remains an area of high production of freezing

during 20 min. From 20 to 40 minutes is produce the maximum quantity of ice, and represents for all profiles the same 20 minutes range.

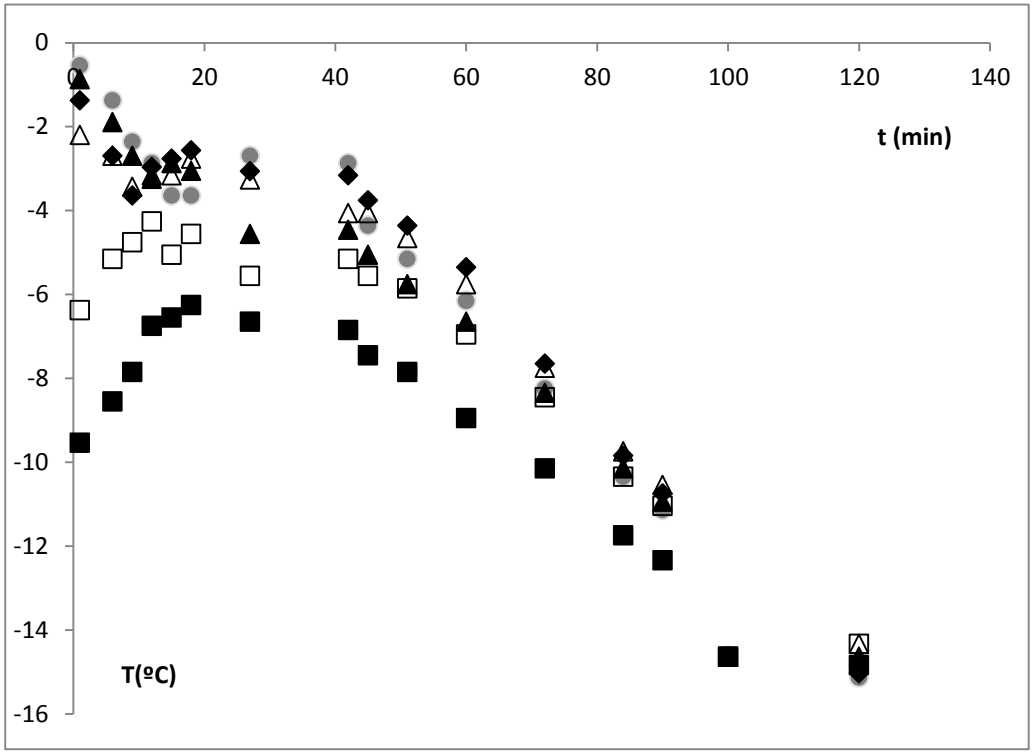

Figure 32 Evolution of Temperature of potato sample through freezing process at 1mm(■), 4mm(□), 5mm(▲), 1cm(Δ), 2cm(♦) and centre (●); being distance (r) beginning in the surface.

Again, there is shown a flux of water from the inner heating the surface, the water flux has to be promoted by the production of ice and the consequent concentration process of the liquid phase.

The water activity of potato through the freezing can be estimate by Robinson & Stokes (1965) adapted by Fontan and Chirife (1981), in next equation (see equation II.6):

$$-ln(a_w) = 9.6934 \cdot 10^{-3} \cdot \Delta T_f + 4.761 \cdot 10^{-6} \cdot \Delta T_f^2 \text{ (eq. II.6)}$$

Being ΔT_f the gradient between the initial freezing temperature and the freezing temperature of product.

The engine of the movement of water is the water chemical potential and it is possible to define as follows (see equation II.7):

$$\mu_w = \mu_w^0 + RTlna_w \text{ (eq. II.7)}$$

Figure 33 shows the evolution of water chemical potential at different distances, where it is possible to observe high gradients close the surface and low gradients close de centre of sample.

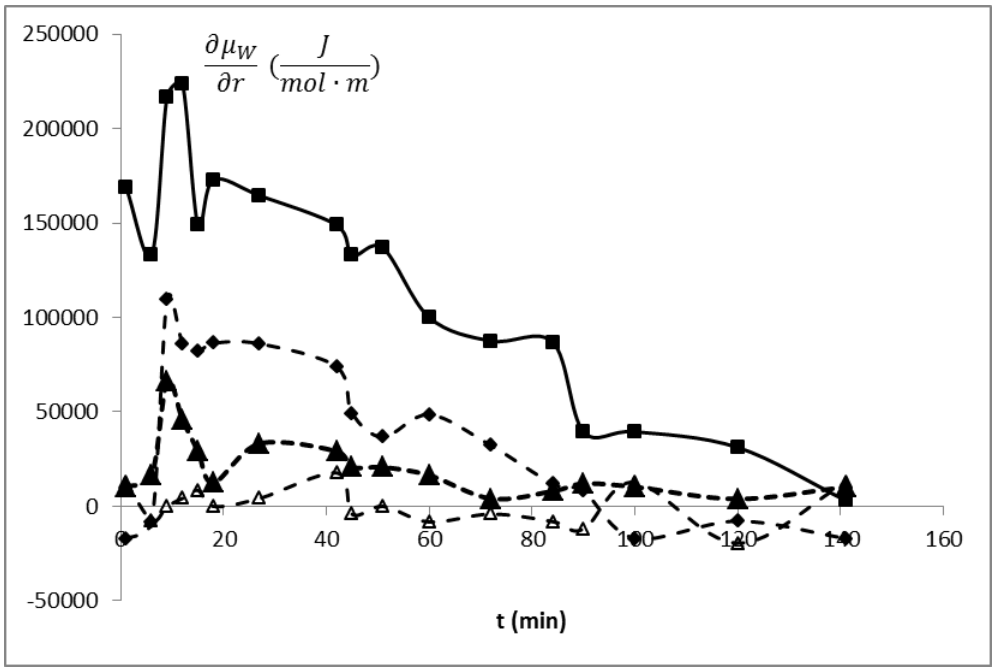

Figure 33 Variation of gradient of chemical potential through the time at surface (♦), 1 mm (■), 2 mm (▲) and 1 cm (Δ).

Water chemical potential promote the water transport from the inside to outside, heating the surface, because the water inside is warmer than the water close the surface. This water transport, accumulate water in a ring close the surface, in a continuous process of ice production. Therefore the water freezing produce an increasing of the overall volume of sample. In *figure 34* is possible to observe the partial volume average of samples throughout the freezing process.

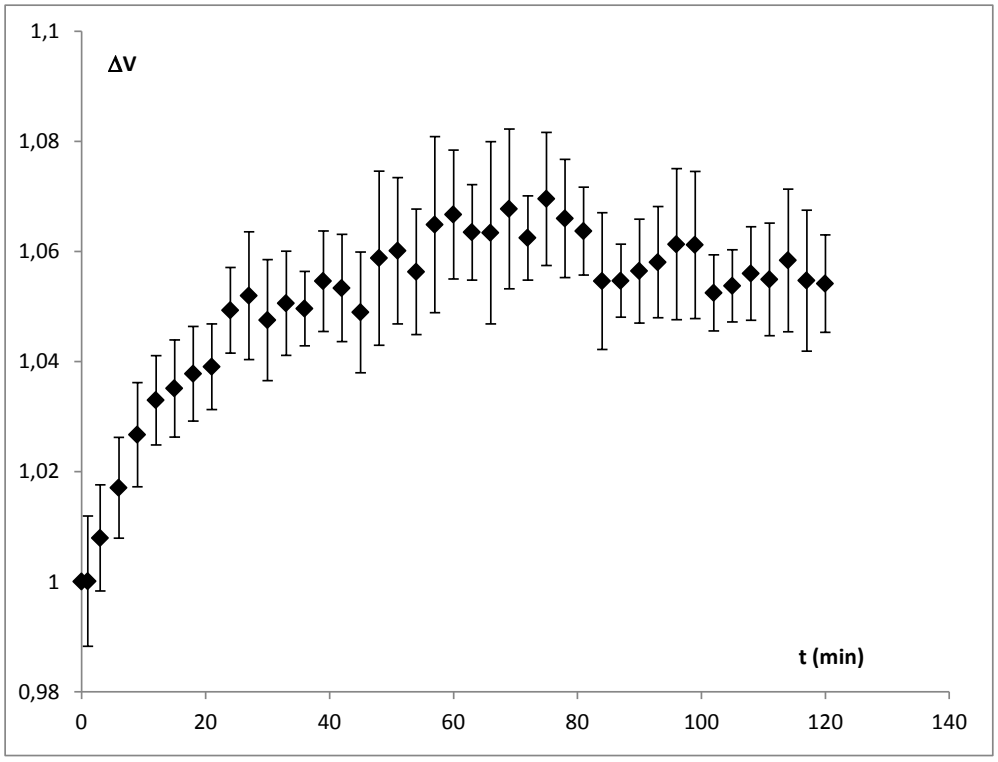

Figure 34 Partial volume increment through the freezing process.

Figure 34 shows how after 40 minutes, the cylinder still grown, reaching the maximum increase at 80 minutes, therefore the ice formation is important till this time, *figure 32*, shows a temperature from -11 to -12 ºC for all profiles. By other hand, with the enthalpy of melting of potato (see **table 5**) obtained from the calorimetric analysis and the enthalpy of melting pure water obtained from the bibliography is possible to obtain the unfreezeable water.

Table 5. Results from the DSC experiments, moisture and non freezeable water estimated

$\Delta H_{melting}$	$\Delta H_{freezing}$	ΔH_{water}	Tm'	x_w^0	x_w^{nf}
223±15	249±19	334	-19±2	0.847±0.015	0.204±0.016

Thus, the freezing process produce ice throughout all process because never reach the Tm', prompting continuous gradients of water chemical potential and consequently water movement, this phenomenon produces ice accumulation in the area near the surface, dehydrating the middle of the samples, preserving the inner area and degrading the area near the surface. *Figure 35* present an scheme explaining the dehydration process with the freezing and the accumulation energy as a freezing latent heat.

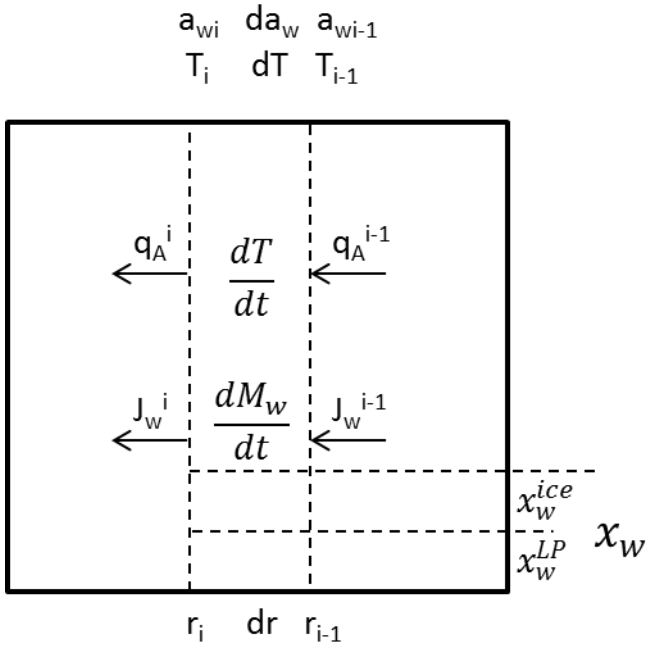

Figure 35 Scheme of heat modelling to predict the behaviours involves in the freezing process.

In the *figure 36* we can see the microstructure of fresh potato cells tissue are intact. The damage of cell structures of tissues, during the freezing process itself can be mainly attributed to alterations of the middle lamella, cell membranes and cell walls (Fennema, Powrie, &Marth, 1973). Though the freezing process, water appears in multi phases, intracellular space, extracellular space, starch globules,

cell organs; the different membranes and layers that produce this separation of water molecules also produce a resistance in the heat transmission. Therefore, the freezing process produces different levels of ice and water liquid concentration with the associated water transport. Water transport produces the deformation of the tissue, as show *figure 33*, a water transport is promoted throughout the freezing, induced by high gradients of water chemical potential, the water transport accumulate ice close the surface of sample and dehydrate (preserving the tissue) in the middle of potato. Comparing the left microstructure of fresh potato, wall and membrane appears with tension; high water content inside de cell produce high internal high pressure (Castro-Giraldez, et al., 2011), right micrographies shows walls and membranes softs with folds, because the water transport reduce the internal pressure.

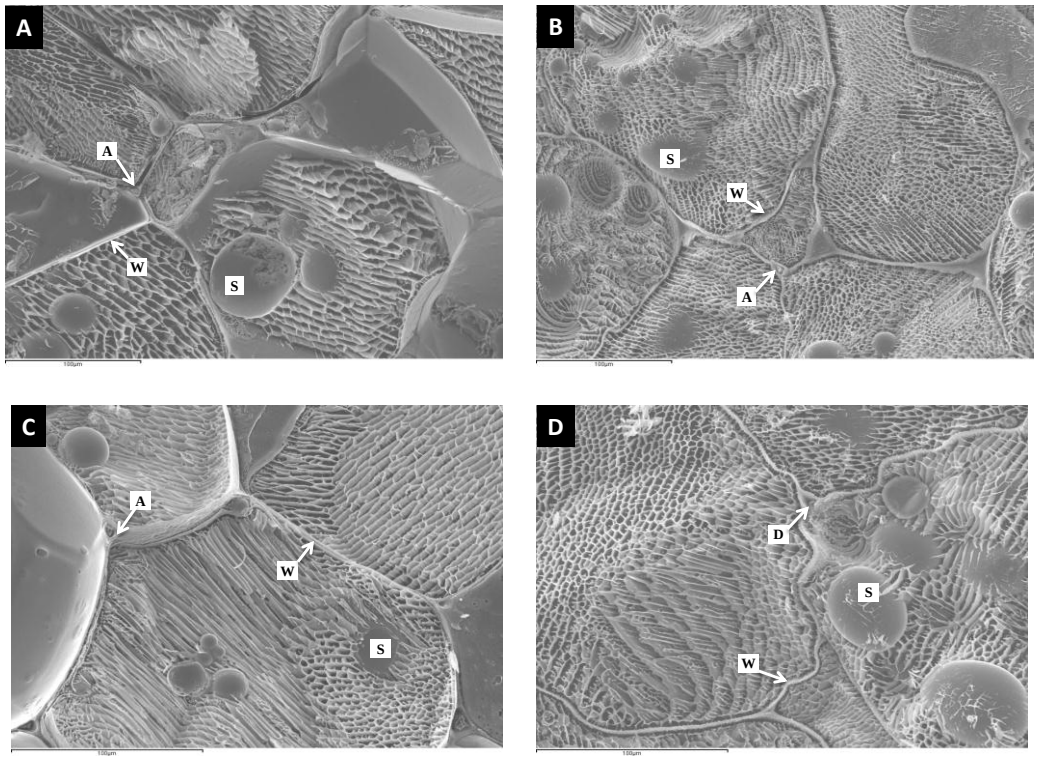

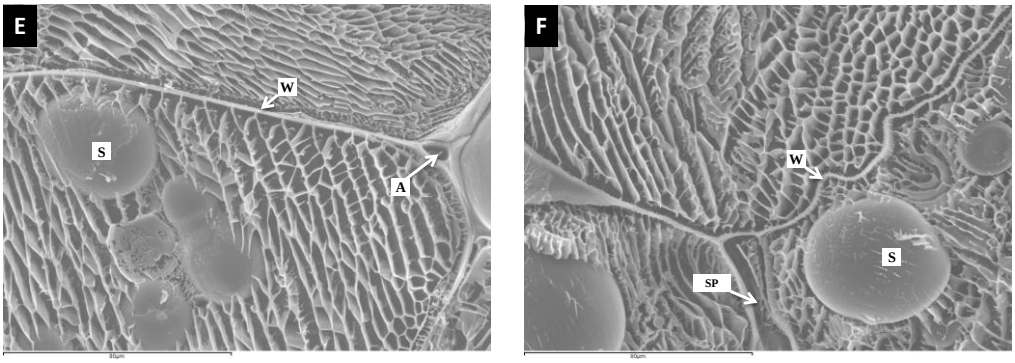

Figure 36 Cryo-SEM micrograph for fresh (A-350x,C-500x,E-750x) and thaw (B-350x,D-500x,F-750x) potato raw tissue (A: air space; S: starch granule; W: cellular wall and membrane structure, SP: separation of cells, D: disruption of cells).

Dielectric properties were measure in the middle of sample, where the dehydration process by freezing were bigger, and were the thawing process recover better the original structure. *Figure 37* shows the spectra and also the average values of loss factor in range of the effect of ionic molecules and in range of water molecules.

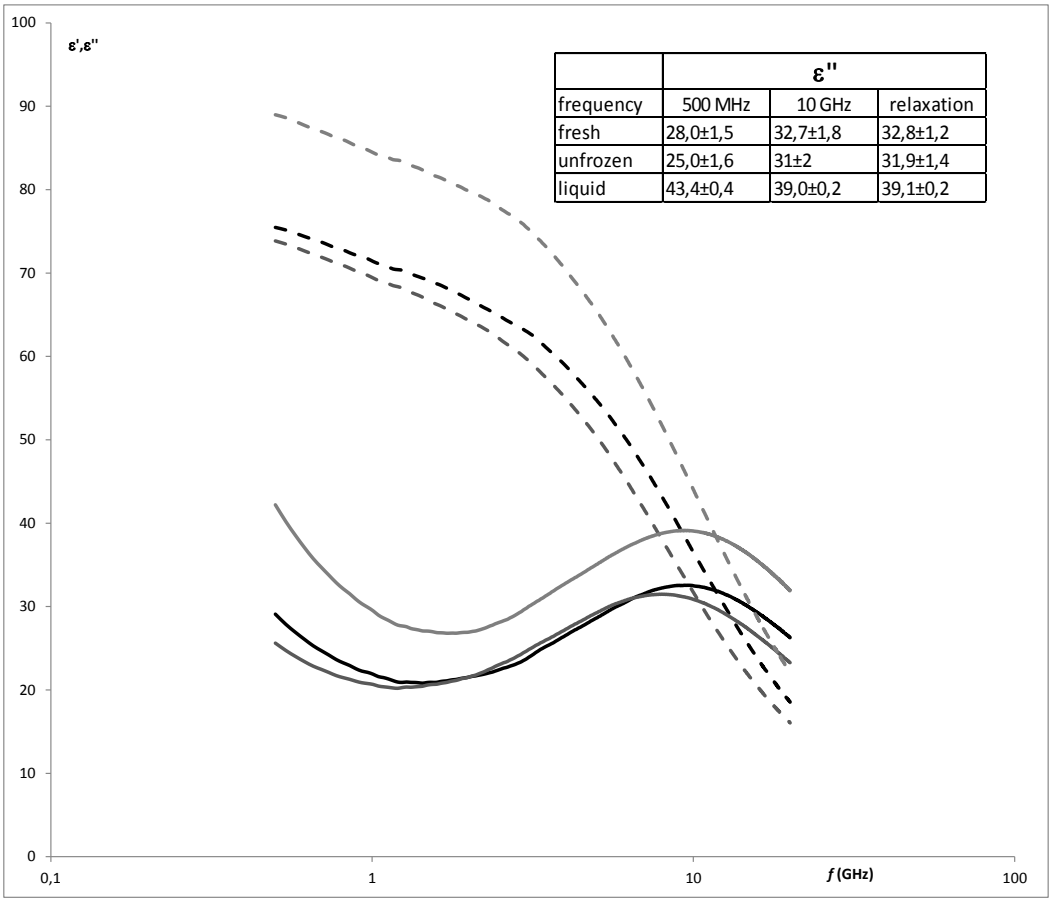

Figure 37 Dielectric spectra of fresh (black line) and thaw potato (dark grey line) and liquid form thawing process (soft grey line); being solid line for loss factor and dashed line for dielectric constant. Table shows the average values of loss factor in range of 500 MHz, 10 GHz and gamma relaxation frequency.

Figure 37 shows in the average values of loss factor how the structure recover the fresh structure in the middle of sample, but It is possible to observe how grown the values in the liquid loss in thawing process with high mobility in the ionic compounds and in the water, produced by the worst structural state in the areas near the surface of the potato.

Conclusions

The freezing process produce ice throughout all process because never reach the Tm', prompting continuous gradients of water chemical potential and consequently water movement, this phenomenon produces ice accumulation in the area near the surface, dehydrating the middle of the samples, preserving the inner area and degrading the area near the surface.

Infrared thermography not only serves to keep the heat fluxes flowing through the potato but in addition also serve to keep the water activity gradients which move this chemical specie by changing the structural state inside thereof.

II.3.4 References

Aguilera, L. M., & Stanley, D. W. (1990). Microstructural principles of food processing and engineering. Essex, UK: *Elsevier Science Publishers Ltd.*

AOAC (1990), *Official methods of analysis* (15th ed.). Association of Official Analytical Chemists, Arlington, VA.

Da-Wen Sun *, Bing Li, (2002). Microstructural change of potato tissues frozen by ultrasound-assisted immersion freezing, *Journal of Food Engineering*

Fellows, P. (2000).Food Processing Technology—Principles and Practice (2nd ed., pp. 418–440). Chichester, UK: *Ellis HorwoodLtd*.

Fuller M. P.&Wisniewski M., (1998). The use of infrared thermal imaging in the study of ice nucleation and freezing of plants *Journal of Thermal Biology* Vol. 23, No. 2, pp. 81-89.

Gowen, A. A., Tiwari, B.K., Cullen, P.J., O'Donnell, C.P., McDonnell, K. (2010). Applications of thermal imaging in food quality and safety assessment.*Trends in Food Science & Technology* 21 (2010) 190e200

Giorleo, G., &Meola, C. (2002). Comparison between pulsed and modulated thermography in glasseepoxy laminates. *NDT & E International*, 35(5), 287e292.

Jalté M., Lanoisellé J.L., Lebovka, N. I., & Vorobiev, E. (2009). Plasmolysis of sugarbeet: pulsed electric fields and thermal treatment. *LWT - Food Science and Technology 42* 576–580

Karlsson, M.E. &Eliasson A.-C. (2003). Gelatinization and retrogradation of potato (Solanum tuberosum) starch in situ as assessed by differential scanning calorimetry (DSC) *Lebensm.-Wiss. u.-Technol*. *36* 735–741

Kita, A. (2002). The influence of potato chemical composition on crisp texture, *Food Chemistry 76*,173-179

Le Grice, P., Fuller, M. P. and Campbell, A. (1993). An investigation of the potential use of thermal imaging technology in the study of frost damage to sensitive crops. *Proceedings of 6th International Conference on Biological Ice Nucleation. University of Wyoming*, Laramie, USA, p. 4.

Li, B., & Sun, D.-W.(2002a). Novel methods for rapid freezing and thawing of foods–A review. *Journal of Food Engineering*, *54*, 175–182.

Li, B.,& Sun, D.-W.(2002b). Effect of power ultrasound on freezing rate during immersion freezing.*Journal of Food Engineering*, *55*, 85–90.

Minkina, W. (2004). Thermovision Measurements – Instruments and Methods, *Publishing Office of Częstochowa University of Technology, Częstochowa,* (in Polish)

Singh, J., Kaur, L. (2009). Advances in potato chemistry and technology, *Academic Press, Elsevier Inc*.

Świędrych, A., Prescha, A., Matysiak-Kata, I., Biernat, J., Szopa, J. (2002). Repression of the 14-3-3 gene affects the amino acid and mineral composition of potato tubers, *Journal of agricultural and Food Chemistry*, 50, 2137-2141

Szymońska, J., &Wodnickab, K. (2005). Effect of multiple freezing and thawing on the surface and functional properties of granular potato starch, *Food Hydrocolloids* ,753–760

II.4 Spinach- Infrared thermography versus image analysis: A survey

II.4.1 Introduction

Spinach (Spinacia oleracea) was recorded in Europe as early as the mid-13th century, with colonists carrying spinach seed to the New World and is native from Southwest Asia. The consumption of spinach increases during the years and this vegetable increases the lymphocyte DNA resistance to oxidative stress (Porrini et al., 2002).

Freezing is an extensively used method for long preservation of food quality products, which may result in textural changes leading to tissue softening. The freeze food product has been increasing in recent years, especially as a result of changes in the lifestyles of consumers (Ragaert et al., 2004). The quality of frozen foods depends on the size of ice crystals (Li & Sun, 2002 a, b) and some attempts have been made to improve the resistance of fruit and vegetables to freezing damage by several methods (Moraga et al., 2006 and Suutarinen et al., 2000). Rapid freezing produces small intracellular ice crystals, but if the product it's kept for a long time frozen, the formed ice crystals expand creating irreversible damage for the cell membrane. Infrared thermography becomes popular and is being used in the agro-food research and processing because of the characteristic non-destructive of this technique to measure the temperature of surface of the products.

The objective of this study was to evaluate the capability of IRT to detect the ice dimension distribution comparing with image analysis system. This paper reports the development of image processing methods for the detection of superficial changes related to quality deterioration in spinach cubes freeze after 10

months of storage at -20 °C. This survey was realized at the end of the one part of the project that study the development of image processing methods for the detection of superficial changes, ice crystal dimension, related to quality deterioration in freeze spinach cubes during storage for a long period. To have a better control of the crystal ice formation the cubes were analyzed every week and see the difference of ice crystal dimensions using a digital camera.

II.4.2. Material and methods

Theorical considerations

The radiance entering a thermographic camera originates from three sources (Lamprecht et al., 2002): (i) the observed object itself; (ii) other objects reflected on the target's surface, and; (iii) an atmospheric contribution.

$$R_T = \varepsilon_r \sigma T_r^4 = \varepsilon_{obj} \sigma T_{obj}^4 + (1 - \varepsilon_{refl}) \sigma T_{refl}^4 + (1 - \tau) \sigma T_a^4 \qquad \text{(II.8)}$$

where R_T is the energy flux emitted at a wavelength of 7.3–13 μm in W m^{-2}, ε is the emissivity of the target (equal to 1 for a perfect emitter), σ is Stefan–Boltzmann's constant (5.67051 × 10−8 W m^{-2} K^{-4}), (1 – ε) corresponds to the reflectivity, (1 – τ) is the emittance of the atmosphere, T is the temperature of the target, T_{refl} is the background temperature that the target is reflecting and T_a is the air temperature, all in K.

With the use of an image capture device such as a digital camera (Nikon D7000), an image can be analyzed by application of the appropriate algorithms to determine some characteristics regarding the structural quality of the products.

Experimental procedure

The Spinach (Spinacia oleracea) cubes freeze used for our experiment was stored at -20 °C for 10 months. The setup of the experiment is shown in the *figure 38*. A black box was used in order to remove light reflections that could have disturbed our measurements. For image analysis was used a digital camera Nikon D7000 (Nikon Corp., Tokyo, Japan) with a professional 105 mm lens. The

settings used for the camera were: exposure time 0.77 sec., ISO 100, f-stop f-16, digital zoom 1, and metering mode was set to spot. The pictures obtained in sRGB format color have a resolution about 4928 x 3264 pixels, 300 dpi, and bit depth 24.

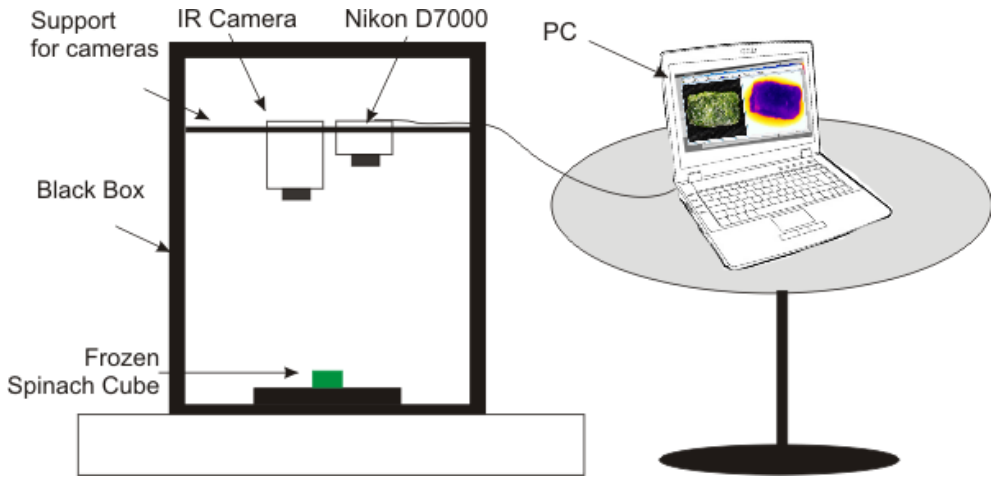

Figure 38 Experimental setup for measuring the ice crystal dimension by Nikon D700 digital camera and Flir A325 infrared thermocamera.

For the measurement of temperature of spinach freeze cubes were use an infrared camera FLIR A325 with a spectral infrared range of wavelength from 7.5 to 13.0 μm, a temperature range of -20 to + 120 °C. The thermograms obtained use the sRGB color representation and a resolution around 320 x 240 pixels, 72 dpi, and bit depth 24. The emissivity used for this measurement was set at 0.98 (Fuchs & Tanner 1966; Salisbury & Milton, 1988; Rahkonen & Jokela 2003). Measurements were performed at ambient room temperature of 22 ± 2°C.

The freeze cubes stored at -20 °C were carried out from the freezer and fix in the black box. After that were captured images using the both camera for 15 samples. The images obtained were analyzed using professional software Image-Pro Plus.

II.4.3. Results and discussion

The highest obstacle in this analysis was the resolution of the pictures that we can see also in the *figure 39*. In the first case the digital image with a highest resolution confers more information and was possible to analyze the dimension of ice crystals.

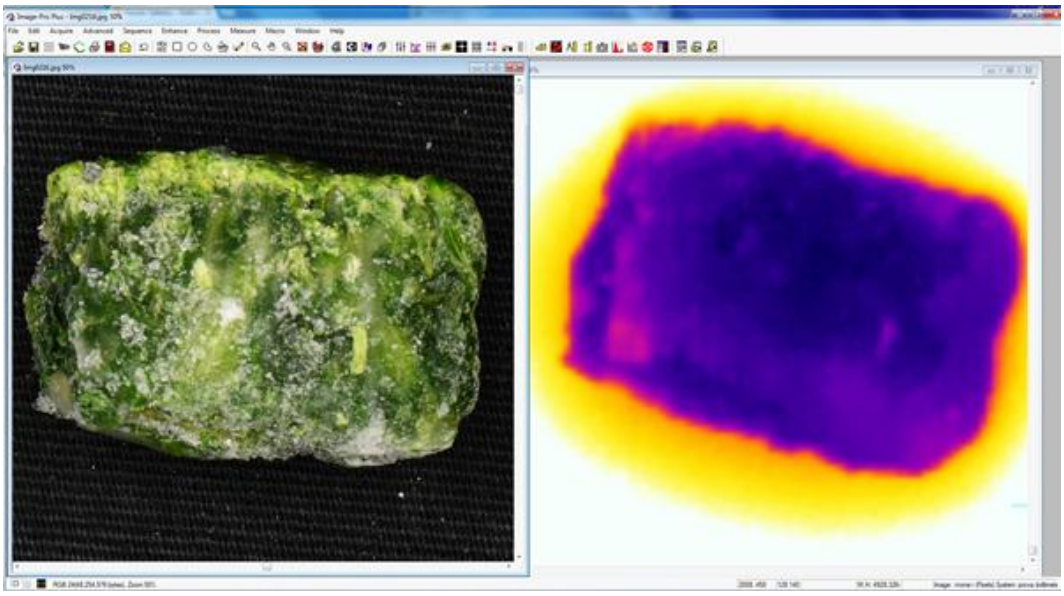

Figure 39 Comparing the RGB digital image with an infrared image using Image-Pro Plus software.

The thermogram having a less resolution doesn't offer enough data to correlate with the dimension of ice crystals. The temperature of the spinach is not very relevant in this case because the spinach cube is covered entirely with ice with a different thickness. In this case any reflection can cause a temperature measurement error. We have tried also to analyze the spinach cubes after defrosting, but in this case we lose a high quantity of ice and the applicability in industrial line are without any benefit.

After the data analysis of the picture obtained we can conclude that is difficult finding a correlation between data from digital image and thermogram am more analysis are required. With the new sensors development with a higher resolution for infrared thermocamera we can confront this 2 techniques.

The techniques available for digital image analysis are applied with success in many control steps in the food industry (i.e., colour, size, shape, and texture). IR images are very adequate for the process where is important to have a control of surface temperature of the product, non-destructive and with a low importance in terms of image resolution.

II.4.4. References

Fuchs,M. , Tanner, C.B. (1966). Infrared thermometry of vegetation. *Agronomy Journal, 58,* 597–601

Lamprecht, I., Schmolz, E., Hilsberg, S., Schlegel, S., (2002). A tropical water lily with strong thermogenic behaviour-thermometric and thermographic investigations on Victoria cruziana. *Thermochimica Acta, 382,* 199–210.

Li, B., & Sun, D.-W. (2002a). Novel methods for rapid freezing and thawing of foods—a review. *Journal of Food Engineering, 54,* 175–182.

Li, B.,& Sun, D.-W. (2002b). Effect of power ultrasound on freezing rate during immersion freezing. *Journal of Food Engineering, 55,* 85–90.

López,A., Molina-Aiz,F.D., Valera, D.L., Peña, A. (2012). Determining the emissivity of the leaves of nine horticultural crops by means of infrared thermography. *Scientia Horticulturae, 137,* 49-58

Moraga, G., Martínez-Navarrete, N., Chiralt A., (2006). Compositional changes of strawberry due to dehydration, cold storage and freezing-thawing process *Journal of Food Processing and Preservation, 30,* 458–474

Porrini M, Riso P, Oriani G. (2002). Spinach and tomato consumption increases lymphocyte DNA resistance to oxidative stress but this is not related to cell carotenoid concentrations. *European Journal of Nutrition 41,* 95-100

Ragaert, P., W. Verbeke, F. Devlieghere, J. Debevere. (2004) Consumer perception and choice of minimally processed vegetables and packaged fruits *Food Qual. Preference, 15,* 259–270

Salisbury,J.W., Milton, N.M. (1988). Thermal infrared (2.5–13.5 μm) directional hemispherical reflectance of leaves. *Photogrammetric Engineering & Remote Sensing, 54*, 1301–1304

Suutarinen, J., Heiska, K., Moss, P, Autio, K. (2000). The effects of calcium chloride and sucrose prefreezing treatments on the structure of strawberry tissues *LWT Food Science and Technology, 33*, pp. 89–102

VERBALE DEL COLLEGIO DOCENTI
DOTTORATO IN INGEGNERIA AGRARIA

Il giorno 07.03.2013 alle ore 19.00 in una sala del Dipartimento di Economia e Ingegneria Agrarie dell'Università di Bologna, si riunisce il Collegio dei Docenti del Dottorato in Ingegneria Agraria.

Risultano presenti: Adriano Guarnieri, Patrizia Tassinari, Marco Bentini, Giuseppe Taglioli, Giorgio Ade, Fabio Pezzi, Giovanni Molari, Angelo Fabbri, Paolo Zappavigna, Luigi Ragni, Donatella Pavanelli, Paolo Liberati, Daniele Torreggiani, Stefano Benni

Risultano assenti giustificati: Valda Rondelli, Antonio Checchi, Claudio Caprara.

Presiede la seduta il: prof. ing. Adriano Guarnieri

Segretario del collegio: prof. ing. Giovanni Molari

ORDINE DEL GIORNO

1. Comunicazioni
2. Presentazione dottorandi XXV da allegare alla tesi
3. Varie

…….OMISSIS…….

2) Presentazione dottorandi XXV Ciclo da allegare alla tesi

Il Collegio è chiamato a redigere, per ciascun allievo, la "presentazione" da allegare alla tesi finale.
Si invitano, a tal fine, i componenti del Collegio, che prevalentemente hanno guidato le attività di ricerca dei dottorandi a voler illustrare i contenuti delle predette tesi ed i risultati conseguiti dagli allievi.
Dopo ampia discussione, il Collegio dei Docenti decide, unanime, di approvare le **"presentazioni**" di seguito riportate che illustrano la personalità di ciascun dottorando e l'attività scientifico - formativa svolta durante il corso, mettendone in luce gli aspetti positivi o, eventualmente, negativi.

Ing. Lucian Cuibus
Curriculum seguito: Macchine e impianti per i prodotti agricoli
Titolo tesi: Applications of infrared thermography in the food industry

L'ing. Lucian Cuibus, nel periodo di attività del dottorato, ha partecipato alle attività formative programmate. Ha svolto attività di ricerca relativa all'applicazione della termografia infrarossa su diversi prodotti alimentari, in termini di miglioramento della qualità e della sicurezza degli alimenti. L'ing. Cuibus si è occupato inoltre della validazione sperimentale di modelli numerici di processi, sviluppati in precedenza, relativi al trattamento termico di uova con aria calda. L'ing. Cuibus ha trascorso un periodo all'estero presso l'Institute of Food Engineering for Development Department of Food Technology, Polytechnic, University of Valencia, Spain, sotto la guida del prof. Pedro J. Fito Suñer. Durante lo stage il dottorando si è occupato di studio della applicazione della termografia al controllo della surgelazione della patata. Ha inoltre svolto attività di supporto alla didattica. Visto il percorso formativo svolto, il collegio dei docenti esprime unanime il parere favorevole all'attribuzione del titolo di Dottore di Ricerca per l'ing. Lucian Cuibus.

…….OMISSIS…….

Le deliberazioni assunte in questa seduta, sono redatte, lette e sottoscritte seduta stante.
La seduta è tolta alle ore 19.45.

IL SEGRETARIO
Prof. Ing. Giovanni Molari

IL PRESIDENTE DELLA SEDUTA
Prof. Ing. Adriano Guarnieri

UNIVERSITAT POLITÈCNICA DE VALÈNCIA

IIAD
INSTITUTO DE INGENIERÍA DE ALIMENTOS PARA EL DESARROLLO

Valencia 9/11/2012

This letter confirms that Student Lucian Cuibus at Department of Agricultural Economics and Engineering, University of Bologna, can use the study data for his Phd thesis, obtained on the research period from 28th of September 2011 to 11th of April 2012, at Institute of Food Engineering for Development of the Universidad Politécnica de Valencia, Spain.

The topic of research was: "Dielectric Spectroscopy and Infrared thermography for controlling different food processes".

Yours sincerely,

Fdo. Pedro J. Fito Suñer

Fdo. Marta Castro Giráldez